



**HAL**  
open science

## Structural, electronic and magnetic properties of some early vs late transition dimetallaborane clusters - A theoretical investigation

Kandasamy Bharathi, Lalshab Beerma, Chinnasamy Santhi, Bellie Sundaram  
Krishnamoorthy, Jean-François Halet

### ► To cite this version:

Kandasamy Bharathi, Lalshab Beerma, Chinnasamy Santhi, Bellie Sundaram Krishnamoorthy, Jean-François Halet. Structural, electronic and magnetic properties of some early vs late transition dimetallaborane clusters - A theoretical investigation. *Journal of Organometallic Chemistry*, 2015, 792, pp.220-228. 10.1016/j.jorganchem.2015.05.057. hal-01158448

**HAL Id: hal-01158448**

**<https://univ-rennes.hal.science/hal-01158448>**

Submitted on 12 Nov 2015

**HAL** is a multi-disciplinary open access archive for the deposit and dissemination of scientific research documents, whether they are published or not. The documents may come from teaching and research institutions in France or abroad, or from public or private research centers.

L'archive ouverte pluridisciplinaire **HAL**, est destinée au dépôt et à la diffusion de documents scientifiques de niveau recherche, publiés ou non, émanant des établissements d'enseignement et de recherche français ou étrangers, des laboratoires publics ou privés.

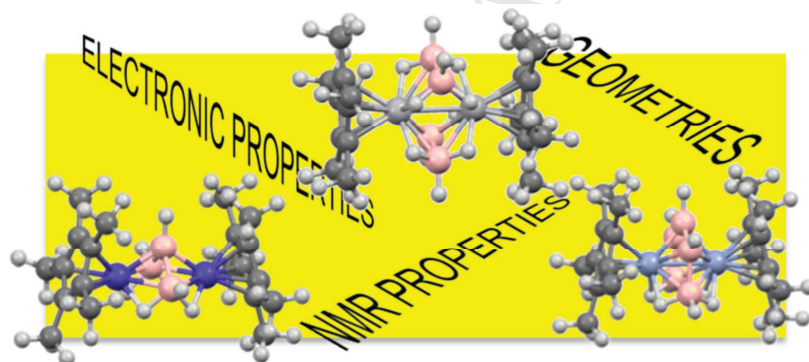
For the table of contents use only

## Structural, electronic and magnetic properties of some early vs late transition dimetallaborane clusters - A theoretical investigation

Kandasamy Bharathi<sup>a</sup>, Lalshab Beerma<sup>a</sup>, Chinnasamy Santhi<sup>a</sup>, Bellie Sundaram Krishnamoorthy<sup>a,b,\*</sup> and Jean-François Halet<sup>b,\*</sup>

<sup>a</sup>*Department of Chemistry, Vivekanandha College of Arts and Sciences for Women (Autonomous), Elayampalayam, Tiruchengode, 600 036, India*

<sup>b</sup>*Institut des Sciences Chimiques de Rennes, UMR 6226 CNRS-Université de Rennes 1, Avenue du Général Leclerc, 35042 Rennes Cédex, France*



## Structural, electronic and magnetic properties of some early vs late transition dimetallaborane clusters - A theoretical investigation

Kandasamy Bharathi<sup>a</sup>, Lalshab Beerma<sup>a</sup>, Chinnasamy Santhi<sup>a</sup>, Bellie Sundaram Krishnamoorthy<sup>a,b,\*</sup> and Jean-François Halet<sup>b,\*</sup>

<sup>a</sup>*Department of Chemistry, Vivekanandha College of Arts and Sciences for Women (Autonomous), Elayampalayam, Tiruchengode, 600 036, India*

<sup>b</sup>*Institut des Sciences Chimiques de Rennes, UMR 6226 CNRS-Université de Rennes 1, Avenue du Général Leclerc, 35042 Rennes Cédex, France*

**ABSTRACT.** The strength of DFT methods in analyzing the electronic and magnetic properties of a series of dimetallaboranes of varied stoichiometry and architectural core, namely  $M_2B_3$ ,  $M_2B_4$  and  $M_2B_5$  with both early- and late-transition metals is demonstrated. In particular, the observed  $^1H$  and  $^{11}B$  chemical shifts of most of the studied compounds are reproduced with a good accuracy of a few ppm at the DFT-GIAO BP86/TZ2P/SC level for the compounds with first-row transition metal elements and at the B3LYP/TZ2P/SO level for those with second- and third-row transition metal elements. This allows structural applications in elucidating the number and the location of bridging hydrogen atoms in experimentally poorly characterized metallaboranes such as  $(Cp^*Cr)_2B_4H_8$ .

Dedicated to Prof. Michael Mingos on the occasion of his 70<sup>th</sup> birthday in recognition of his major contributions to cluster chemistry.

**Keywords:** Cluster compounds . Density functional theory . Metallaborane complexes. NMR spectroscopy

\* Corresponding authors. *E-mail addresses:* bskimo@yahoo.co.in (B. S. Krishnamoorthy) and halet@univ-rennes1.fr (J. -F. Halet)

## Introduction

Although the proven methods for the formation of compounds containing metal-boron bonds are rather limited, there are today a plethora of metallaborane compounds, which have been synthesized and characterized with nearly all the transition metals, early and late metals [1]. Among them, dimetallaboranes constitute a larger part, with almost one hundred of them known and structurally and/or spectroscopically characterized [2-22]. Although the chemistry of these dimetallaboranes is experimentally growing rapidly, theoretical studies on these species are still rather scarce, despite the need to investigate and rationalize viz., (i) their structural diversity, (ii) their thermal and kinetic stability, (iii) their isomeric preferences, (iv) their chemical bonding, (v) their spectroscopic properties, etc. In particular, quantum chemical computations of  $^{11}\text{B}$  and  $^1\text{H}$  NMR chemical shifts have become one of the principal means of characterization of metallaborane compounds. These computations can even sometimes “rival that of X-ray crystallography” [24]. Density-functional theory (DFT) computations for instance can nowadays provide usefully precise chemical shifts as a function of the geometrical structure [25]. This has been shown by the past for some metallacarboranes for instance [26,27]. Recently, we have used such methods to tackle with some success the structural, electronic, and NMR properties of specific examples of dimetallaboranes [29-32].

For the latter, accuracies of about 2 to 3 ppm were achieved for the computed  $^{11}\text{B}$  chemical shifts at the B3LYP/TZ2P all-electron relativistic scalar ZORA level of theory. Indeed, we have shown that although they are very computationally demanding,  $^{11}\text{B}$  NMR chemical shift calculations at this level of theory using BP86/TZ2P/SC optimized geometries improves

considerably (by ca. 5-10 ppm) the computed values with respect to those obtained at the GGA/TZ2P all-electron relativistic scalar ZORA level, for early *4d* transition metal-borane systems (dimolybdaboranes, ditantalaboranes) [29,30]. On the other hand, only 1-2 ppm of improvement is observed for the metallaboranes with late *4d* transition metal (diruthenaboranes for instance) [31]. This drove us to look at the suitability of DFT methods using different GGA vs. hybrid functionals to accurately compute  $^{11}\text{B}$  NMR chemical shifts in metallaboranes in general. For this purpose a series of dimetallaboranes of varied stoichiometry and architectural cores, namely  $\text{M}_2\text{B}_3$ ,  $\text{M}_2\text{B}_4$  and  $\text{M}_2\text{B}_5$ , with early and late transition metals has been chosen and studied (Chart 1). It would have been desirable to compare results on early- and late-transition-metal boranes with the same architecture, but it has been shown experimentally that early transition metals often lead to the formation of rather highly condensed metallaborane clusters (of  $\text{M}_2\text{B}_4$  and  $\text{M}_2\text{B}_5$  core), such as compounds **1-9** (Chart 1) discussed in this work, for example [13,33,34] whereas late-transition elements usually form stable metallaboranes with more open structures (with  $\text{M}_2\text{B}_3$  core), such as compounds **15-17** (Chart 1) discussed in this work, for example [35]. Here we report that the observed  $^{11}\text{B}$  NMR chemical shifts are reproduced with a reasonable accuracy at the BP86/TZ2P/SC level for the *3d* metallaboranes. On the other hand, the B3LYP/TZ2P/SO level (SO = spin-orbit) is necessary for *4d* and *5d* metallaboranes using BP86-optimized molecular geometries. This suggests that this particular combination of DFT levels is suitable for metallaboranes in general.

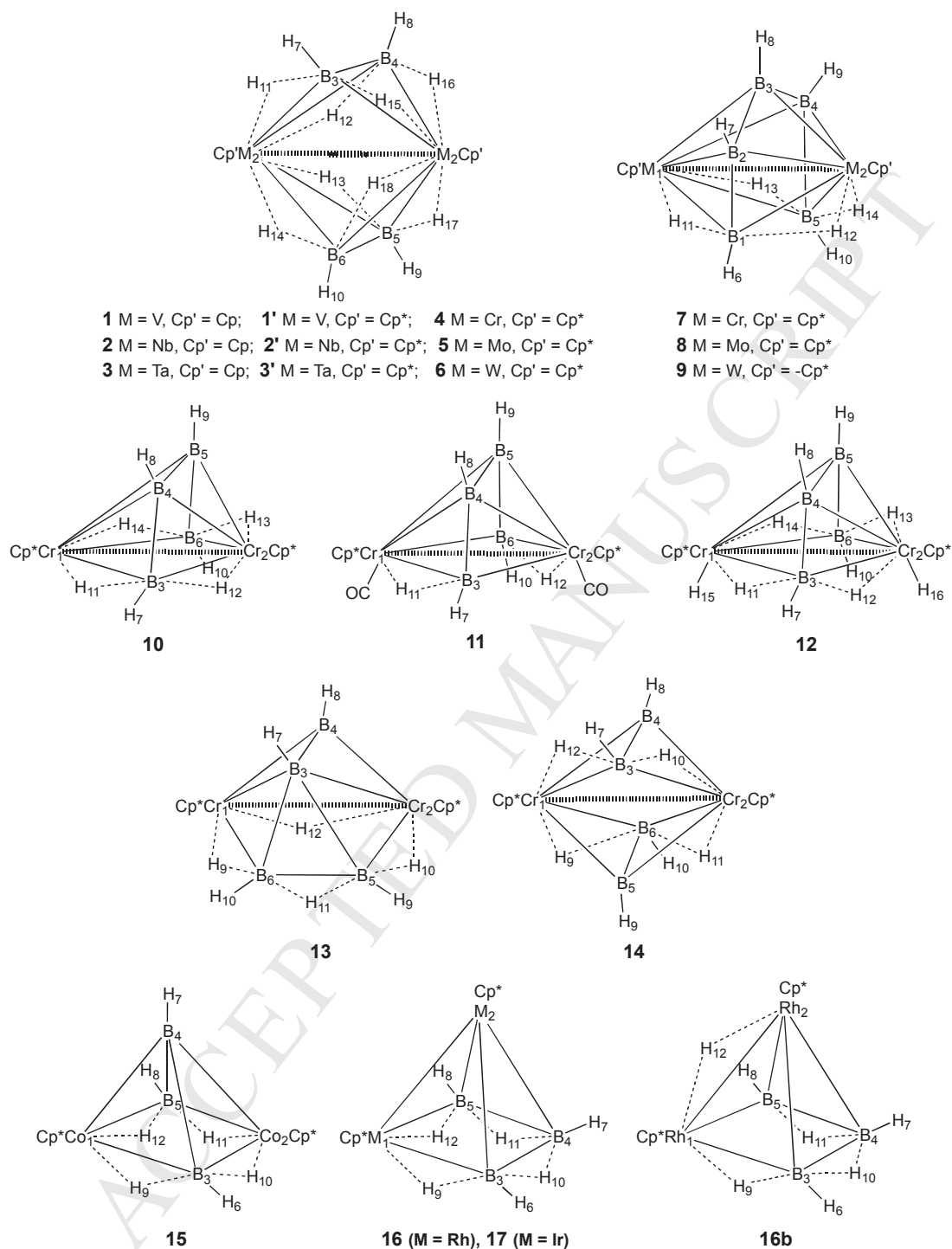


**Chart 1.** Examples of  $M_2B_3$ ,  $M_2B_4$  and  $M_2B_5$  dimetallaborane cluster compounds.

## Computational details

Density functional theory calculations were carried out using the Amsterdam Density Functional (ADF) program [36] developed by Baerends and co-workers [37]. The Vosko-Wilk-Nusair parameterization [38] was used for the local density approximation (LDA) with gradient corrections for exchange (Becke88) [39,40] and correlation (Perdew86) [41]. The geometry optimization procedure was based on the method developed by Versluis and Ziegler [42]. Relativistic corrections were added using the ZORA (zeroth order regular approximation) scalar Hamiltonian [43-45]. Structures were optimized using an all-electron TZ2P basis sets [36], available in the ADF program without any geometrical constraint. Experimental geometries were taken as inputs for compounds when they were available. The nature of the stationary points after optimization was checked by calculations of the harmonic vibrational frequencies to ensure that genuine minima were obtained.

The BP86/TZ2P optimized geometries were then used as inputs for the NMR computations using all-electron TZ2P basis sets [36,38] at the relativistic scalar (SC) ZORA level of theory. NMR chemical shifts were also calculated with the hybrid Becke-Lee-Yang-Parr (B3LYP) functional [46-48] for comparison, using the BP86/TZ2P optimized geometries. The computation of the NMR shielding tensors employed gauge-including atomic orbitals (GIAOs) [49-52], using the implementation of Schreckenbach, Wolff, Ziegler, and co-workers [53-57]. NMR calculations were performed including the spin-orbit (SO) term with both BP86 and B3LYP functionals. TMS ( $\text{SiMe}_4$ ) was used as an internal standard for the  $^1\text{H}$  NMR. The projected  $^{11}\text{B}$  chemical shielding values, determined from relativistic scalar ZORA calculations were referenced to  $\text{B}_2\text{H}_6$  as the primary reference point, and these chemical shift values ( $\delta$ ) were then converted to the standard  $\text{BF}_3\cdot\text{OEt}_2$  scale using the experimental value of +16.6 ppm for  $\text{B}_2\text{H}_6$ .

## Results and discussion

### *Geometries*

Precise structural arrangements are necessary for getting accurate  $^{11}\text{B}$  and  $^1\text{H}$  NMR chemical shifts [58]. Different  $\text{M}_2\text{B}_3$ ,  $\text{M}_2\text{B}_4$  and  $\text{M}_2\text{B}_5$  clusters were then geometrically optimized and compared to experimental data where available. We commence with the  $(\text{Cp}'\text{M})_2(\text{B}_2\text{H}_6)_2$  cluster compounds ( $\text{Cp}' = \text{C}_5\text{H}_5$  (Cp) or  $\text{C}_5\text{Me}_5$  (Cp\*);  $\text{M} = \text{V}, \text{Nb}, \text{Ta}$ ). Salient optimized geometrical parameters are collected in Table 1. The three representatives with Group 5 metals were characterized crystallographically and spectroscopically with either Cp in the cases of  $(\text{CpV})_2(\text{B}_2\text{H}_6)_2$  (**1**) [59] and  $(\text{CpNb})_2(\text{B}_2\text{H}_6)_2$  (**2**) [59] or Cp\* in the case of  $(\text{Cp}^*\text{Ta})_2(\text{B}_2\text{H}_6)_2$  (**3'**) [59]. Overall, the optimized bond lengths reproduce the X-ray data rather well, within a few hundredths of Å, a degree of agreement which is typical for the DFT level employed. The computed M-M bond distances of 2.735 Å, 2.954 Å, and 2.941 Å are comparable to the corresponding X-ray values of 2.787(2) Å, 2.948(16) Å, and 2.933(4) Å, respectively, for clusters **1**, **2** and **3'**. The average M-B bond lengths in these compounds of 2.269 Å, 2.405 Å, and 2.387 Å are substantially longer than the sum of the M and B covalent radii, i.e., 2.20 Å, 2.22 Å, and 2.22 Å for V-B, Nb-B, and Ta-B, respectively [60], supporting the presence of hydrogen atoms bridging M-B bonds. Comparing the computed and experimental B-B bond lengths indicates that the computed ones are 0.02 Å longer for **1** and **3'**, but 0.04 Å shorter for **2**. Finally, we note that geometries computed either with Cp or Cp\* as ancillary ligands attached to the metal atoms are highly similar.

For the Group-6 metal triad, only the molecular structures of  $(\text{Cp}^*\text{Mo})_2(\text{B}_2\text{H}_6)_2$  (**5**) and  $(\text{Cp}^*\text{W})_2(\text{B}_2\text{H}_6)_2$  (**6**) were proposed with an arrangement similar to that encountered for the



Group-5 metal triad discussed above, on the basis of the  $^{11}\text{B}$ ,  $^1\text{H}$  NMR and mass spectrometry details [19,20]. They were computed as well as the hypothetical Cr homolog  $(\text{Cp}^*\text{Cr})_2(\text{B}_2\text{H}_6)_2$  (**4**). BP86/TZ2P optimized geometries show M-M bond lengths of 2.760 Å, 2.900 Å, and 2.909 Å for compounds **4**, **5**, and **6**, respectively (Table 1). The latter for instance is notably longer than the W-W bond length of 2.8174(8) Å reported for  $(\text{Cp}^*\text{W})_2\text{B}_5\text{H}_9$  for instance [19,20], but still short enough to indicate some significant metal-metal bonding interactions at first sight. The rather long computed average M-B bond lengths (2.4015 Å for W-B for instance compared to 2.239 Å in  $(\text{Cp}^*\text{W})_2\text{B}_5\text{H}_9$ , vide infra) may be due to the presence of eight bridging hydrogen atoms. The B-B bond lengths in compounds **4**, **5** and **6** are considerably shorter (1.671 Å, 1.690 Å, 1.686 Å) than normal B-B single bonds observed for the related compounds **1-3** (ca.1.75 Å), reflecting strong B-B bonding interactions in these clusters.

For the *oblato-nido* clusters  $(\text{Cp}^*\text{M})_2\text{B}_5\text{H}_9$  (M = Cr (**7**), Mo (**8**), W (**9**)), the core of which depicts a hexagonal bipyramid with one missing equatorial vertex, the BP86/TZ2P/SC optimized geometries are in good agreement with the metrical parameters measured experimentally by X-ray crystallography (see Table ST1, Supporting Information). The computed M-M bond distances of 2.592 Å, 2.810 Å and 2.835 Å nicely reproduce the experimental ones which are 2.625(9) Å [15], 2.8085(6) Å [30], and 2.817(8)Å [19,20] for **7**, **8**, and **9**, respectively. They indicate significant metal-metal bonding interactions in these clusters.

As said above, the Cr compound  $(\text{Cp}^*\text{Cr})_2(\text{B}_2\text{H}_6)_2$  (**4**) has not been reported so far. With a  $\text{Cr}_2\text{B}_4$  core, the compound  $(\text{Cp}^*\text{Cr})_2\text{B}_4\text{H}_8$  (**10**) has been characterized instead with a *nido* pentagonal bipyramidal cage with one missing equatorial vertex and the two Cr atoms occupying the axial positions and separated by 2.870(2) Å (Chart 1) [61]. The reaction of **10** with CO yielded  $(\text{Cp}^*\text{Cr})_2\text{B}_4\text{H}_6(\text{CO})_2$  (**11**, Chart 1) as the major product [14]. The same *nido* pentagonal

bipyramidal  $\text{Cr}_2\text{B}_4$  cage was confirmed by an X-ray analysis with a Cr-Cr bond length 2.792(1) Å [14]. A DFT geometry optimization of **10** at the BP86/TZ2P/SC all-electron scalar ZORA level resulted in a structure with a Cr1-Cr2 bond length abnormally short of 2.548 Å (Table 2), suggesting that the chemical formula of **10** reported experimentally might be wrong (hydrogen atoms were not directly located from the X-ray analysis [14]). Due to the large difference with the experimental value (0.322 Å), two hydrogen atoms bridging the Cr1-B4 and Cr2-B5 vectors were added (see **10** in Chart 1). The optimized structure resulted in the B3-B4 bond breakage. The two hydrogen atoms were then terminally added to two Cr atoms analogously to the CO ligand in **11**. Interestingly, the optimized geometry of this model structure  $(\text{Cp}^*\text{Cr})_2\text{B}_4\text{H}_{10}$  (see **12** in Chart 1) revealed a  $\text{Cr}_2\text{B}_4$  open cage similar to that computed for **10** but with a Cr1-Cr2 bond length considerably longer of 2.7356 Å, still 0.13 Å shorter than the experimental value experimentally measured for  $(\text{Cp}^*\text{Cr})_2\text{B}_4\text{H}_8$  (**10**) but relatively close to the Cr-Cr bond length experimentally observed in  $(\text{Cp}^*\text{Cr})_2\text{B}_4\text{H}_6(\text{CO})_2$  (**11**), 2.792(1) Å which compares rather well to the computed distance of 2.764 Å (Table 2). The comparison of the computed B-B distances in **10** and **12** with those reported experimentally, are not much informative about the ‘right’ formula. The B3-B4, B4-B5, B5-B6 distances of **10** are 1.735, 1.637, 1.725 Å, respectively, whereas those in the model compound  $(\text{Cp}^*\text{Cr})_2\text{B}_4\text{H}_{10}$  **12**, are 1.701, 1.639, 1.702 Å, respectively. They all deviate somewhat from the corresponding experimental (not very precise) X-ray values which are 1.75(3), 1.75(3), 1.61(3) Å, respectively. Notably, the  $\text{Cp}^*$  ligands are not parallel but tilted away from the open face of the cluster cage with angles of 28.1(8)° and 30.4(20)° experimentally measured for **10** and **11**, respectively [14,61,63]. Interestingly, the  $\text{Cp}^*$  rings are hardly tilted in the optimized geometry of **10** but significantly tilted in **11** and **12** (16° and 14°, respectively). Additional structural arrangements can be envisaged for this compound,

such as a capped square pyramidal (**13**) or  $(\text{Cp}^*\text{Cr})_2(\text{B}_2\text{H}_4)_2$  (**14**) structures with symmetrical  $(\text{B}_2\text{H}_4)$  units (Chart 1) [61]. Their geometry optimization results in Cr-Cr bond lengths of 2.22 and 2.42 Å, respectively. That in the former is comparable to the Cr-Cr triple bond of 2.200(3) encountered in  $\text{Cp}_2\text{Cr}_2(\text{CO})_4$  [64] for instance.

The late-transition metal borane compounds of formula  $(\text{Cp}^*\text{M})_2\text{B}_3\text{H}_7$  have been crystallographically characterized for  $\text{M} = \text{Co}$  (**15**) [5] and  $\text{Rh}$  (**16**) [7] (Chart 1). They display a square pyramidal geometrical cage with two metal atoms occupying basal positions in the case of **15** (*nido*-2,4- $(\text{Cp}^*\text{Co})_2\text{B}_3\text{H}_7$ ) and one metal atom occupying the apical position and the second metal atom occupying one basal position in the case of **16** (*nido*-1,2- $(\text{Cp}^*\text{Rh})_2\text{B}_3\text{H}_7$ ). Interestingly, there is an M-M bond in the latter but not in the former. A tautomer of **16**, i.e., *nido*-1,2- $(\text{Cp}^*\text{Rh})_2(\mu\text{-H})\text{B}_3\text{H}_6$  (**16b**) was also spectroscopically observed [7]. The optimized distances are in a rather good agreement with the experimentally available X-ray values (Table 2, Table ST3, Supporting Information). The computed Rh-Rh bond length in **16** is 2.740 Å, 0.05 Å larger than the X-ray value of 2.6892(3) Å [7]. This deviation might be attributed to the presence of two independent molecules in the unit cell, with a disordered  $\text{Cp}^*$  ring in one molecule, and the fully disordered second molecule, observed in the solid state X-ray structure [7]. This distance is notably shorter than the Rh-Rh bond length of 2.8478(11) Å reported for the *nido*-2,4- $(\text{Cp}^*\text{Rh})_2\text{B}_3\text{H}_6$  Cl cluster for which the two rhodium atoms occupy two adjacent basal positions [7]. Geometry optimization of **16b** results in an intermediate Rh-Rh bond length of 2.744 Å. A very small energy difference, 0.26 kcal/mol, is computed between tautomers **16** and **16b** in favor of the former. The iridium analogue  $(\text{Cp}^*\text{Ir})_2\text{B}_3\text{H}_7$  (**17**) has not been isolated until now. BP86/TZ2P metrical parameters computed with the same arrangement as its Rh congener **16** are comparable to those measured in related diiridium cluster compounds [8]. For example,

the computed Ir-Ir bond length of 2.7733 Å is somewhat shorter than that in *arachno*-(Cp\*IrH)<sub>2</sub>(μ-H)B<sub>2</sub>H<sub>5</sub> which is 2.8227(8) Å [8] but similar to the value of 2.7814(9) Å measured in *arachno*-(Cp\*IrH)<sub>2</sub>B<sub>4</sub>H<sub>8</sub> [8].

#### *Electron counts and electronic structures*

Dimetallaboranes of the earlier transition metals often present interesting challenges to the well-established cluster electron-counting rules, the so-called Polyhedral Skeletal Electron Pair Theory (PSEPT) [65,70], due to their distinctly oblate (flattened along the M-M cross-cluster axis) rather than closely spherical nature [1,13,71,72]. They are generally characterized with short metal-metal cross-cluster distances and *apparent* formal cluster electron counts a few skeletal electron pairs (sep) less (generally three) than required for canonical *closo*- or *nido*-structure of the same nuclearity. Previous DFT calculations suggested that these *oblato* arrangements are indeed very stable compounds, due to an intricate mutual interaction of the dimetal fragment and the borane cage. Indeed, some of us showed that bringing two CpM or Cp\*M fragments close together generates a set of three frontier metal orbitals that can only interact with the frontier orbitals of the borane fragment. These orbitals on each of these complementary fragments, which normally would be filled in a late transition-metal metallaborane with a spherical deltahedral shape, interact strongly to generate three low-lying filled orbitals and three high-lying unfilled orbitals. As a result, they generate a metal-metal cross-cluster bonding where the *effective* sep counts ( $p + 1$  (*oblato-closo*),  $p + 2$  (*oblato-nido*),  $p + 3$  (*oblato-arachno*) if  $p$  is the number of occupied vertices) is three seps larger than the *apparent* sep count obtained via the classical PSEPT [1,13,73].

If these PSEPT-extended rules are applied to compounds **1-3** and **1'-3'**, they can be viewed as *oblato-arachno* species with a structure derived from an 8-vertex *oblato-closo* hexagonal bipyramidal cluster encountered for the effective 9-sep cluster  $(\text{Cp}^*\text{Re})_2\text{B}_6\text{H}_4\text{Cl}_2$  [13], with two non-adjacent vacant sites. Indeed, they have the same effective sep count of 9 ( $[-2 (\text{Cp}^*\text{M}) \times 2 + 2 (\text{BH}) \times 4 + 1 (\text{bridging H}) \times 8 + 6 (t_{2g} \text{M}_2)] / 2$ ), in agreement with a somewhat short metal-metal cross-cluster bond. Surprisingly enough, clusters **4-6** with the same *oblato-arachno* hexagonal bipyramidal core possess an effective sep count of 10 ( $[-1 (\text{Cp}^*\text{M}) \times 2 + 2 (\text{BH}) \times 4 + 1 (\text{bridging H}) \times 8 + 6 (t_{2g} \text{M}_2)] / 2$ ), i.e., one more than the expected electron count. In the same manner, clusters **7-9** can be viewed as *oblato-nido*  $\text{M}_2\text{B}_5$  species also derived from an 8-vertex *closo* hexagonal bipyramidal cluster, possessing the expected effective sep count of 9 ( $[-1 (\text{Cp}^*\text{M}) \times 2 + 2 (\text{BH}) \times 5 + 1 (\text{bridging H}) \times 4 + 6 (t_{2g} \text{M}_2)] / 2$ ).

With only 8 hydrogen atoms cluster  $(\text{Cp}^*\text{Cr})_2\text{B}_4\text{H}_8$ , **10** possesses 8 sep's ( $[-1 (\text{Cp}^*\text{Cr}) \times 2 + 2 (\text{BH}) \times 4 + 1 (\text{bridging H}) \times 4 + 6 (t_{2g} \text{M}_2)] / 2$ ), the expected count if it is assumed that the  $\text{Cr}_2\text{B}_4$  core depicts an open *nido* pentagonal bipyramidal cage. This implies that the carbonyl analog **11** which adopts the same polyhedral cage, has 9 sep's, i.e., one more than expected. A close examination of the X-ray structures of **10** and **11** and the optimized geometries of **10-12** (B3-B4-B5 bond angles and non-bonded B3-B6 distance) indicates that in turn, **10** and **11** are better considered as *oblato-arachno* hexagonal bipyramidal clusters, deriving from an 8-vertex *closo* hexagonal bipyramid by removal of two adjacent basal vertices. Consequently, **10** is an electron-deficient species, whereas **11** (and **12** which possesses 10 hydrogen atoms) possess the expected count of sep's. Fehlner et al. already noted the electronic unsaturation of **10** on the basis of its reactivity and a molecular orbital analysis using semi-empirical Fenske-Hall calculations [63]. The model clusters **13** and **14** [61,62] also result in an effective sep count of five. The shortage of

skeletal electrons in cluster **14** is compensated by a formal Cr-Cr triple bond and thus, in some ways, related to the two-electron richer  $(\text{CpNbCO})_2(\text{RCCR})_2$  compound (M=M double bond) as theoretically pointed out by Hoffmann and colls. [74].

Satisfactorily, all late-transition metal compounds **15-17** with a *nido* square pyramidal  $\text{M}_2\text{B}_3$  cage and a 7-sep count ( $[2(\text{Cp}^*\text{M}) \times 2 + 2(\text{BH}) \times 3 + 1(\text{bridging H}) \times 4] / 2$ ) obey the classical PSEPT rules, as expected.

When dealing with electron counting, it is of major importance not to forget that all the rules, which govern the structure/electron count relationship, are based on the so-called the ‘closed-shell principle’ [1,73]. In other words, these stable dimetallaboranes should exhibit a significant highest occupied molecular orbital (HOMO)–lowest unoccupied molecular orbital (LUMO) energy gap. Indeed, BP86/TZ2P/SC HOMO-LUMO gaps of ca. 2 eV are computed for many of the studied compounds in agreement with their electron counts (Table ST4, Supporting Information).  $(\text{Cp}^*\text{Cr})_2(\text{B}_2\text{H}_6)_2$  (**4**) has not been isolated yet and its heavier congeners **5** and **6** have only been characterized in solution [19,20]. They are too much electron-rich by one extra sep according to the PSEPT-extended rules (see above). Accordingly, a small HOMO-LUMO gap of only 0.71 eV was computed for the non-reported species **4**. Larger energy gaps of 1.42 and 1.51 eV were computed for **5** and **6**, respectively. For the ‘unsaturated’ cluster **10**, a small HOMO-LUMO gap of only 0.65 eV, which does not militate for its existence, led us to look into the details of the structure. A HOMO-LUMO gap of 1.64 eV is computed for **11** which has two electrons more. With two hydrogen atoms more, the HOMO-LUMO gap jumps to 2.21 eV for model **12**, isoelectronic to **11**. Additionally, HOMO-LUMO gaps of 1.57 and 0.98 eV are computed for the model compounds **13** and **14**, respectively. Obviously, these results render the formula of **10** questionable.

*NMR chemical shifts*

The number of direct metal–boron and boron–boron bonds, the presence or absence of bridging hydrogen atoms, the metal identity, the atomic coordination number, the atom charges are some parameters which may influence  $^1\text{H}$  and  $^{11}\text{B}$  NMR chemical shifts in metallaboranes [58].  $^{11}\text{B}$ ,  $^1\text{H}$  and  $^{13}\text{C}$  NMR chemical shifts were calculated at the DFT level using both BP86 and hybrid B3LYP functionals, with and without scalar spin-orbit (SO) relativistic corrections, using BP86 optimized geometries. Data are collected in Tables 3-5 and Tables ST5 and ST6 (Supporting Information) together with the experimental values where available. It turns out overall that the B3LYP/TZ2P/SO ZORA calculated isotropic magnetic shielding constants (converted to  $^{11}\text{B}$ ,  $^{13}\text{C}$  and  $^1\text{H}$  NMR chemical shifts) agree very well with experimental data for clusters with the second and third row early-transition metals Nb, Ta, Mo and W, whereas BP86/TZ2P/SC computed values are in a better agreement for the clusters containing the first row early-transition metals V and Cr. The importance of both scalar and spin-orbit relativistic corrections for the shielding tensors in heavy transition metal complexes was observed previously by Autschbach et al. [75]. Bridging hydrogen atoms in these clusters are relatively shielded and resonate around -6 to -12 ppm.

A single  $^{11}\text{B}$  NMR resonance is experimentally observed at 1.7 ppm for  $(\text{CpV})_2(\text{B}_2\text{H}_6)_2$  (**1**) and  $(\text{CpNb})_2(\text{B}_2\text{H}_6)_2$  (**2**) and at -4.0 ppm for  $(\text{Cp}^*\text{Ta})_2(\text{B}_2\text{H}_6)_2$  (**3'**), revealing the symmetrical nature of these structures in solution [59]. DFT calculations also predict the symmetrical nature of these clusters. In the case of **1**, the  $^{11}\text{B}$  NMR chemical shifts computed at the BP86/TZ2P and B3LYP/TZ2P levels deviate downfield from the experimental values only by 4 ppm for the former but 17.5 ppm for the latter (Table 3). For the carbon atoms of the Cp ligands, a reverse



situation, but less pronounced is computed with a maximum deviation of 6 ppm upfield at the BP86/TZ2P/SC level and only 1 ppm at the B3LYP/TZ2P/SC level when compared to the experimental  $^{13}\text{C}$  NMR chemical shifts. On the other hand, both BP86/TZ2P/SC and B3LYP/TZ2P/SC computed  $^1\text{H}$  NMR chemical shift values are in good agreement with the experimental ones with a maximum deviation of 1 ppm. For **2**, the more accurate  $^{11}\text{B}$  NMR chemical shifts are computed at the B3LYP/TZ2P/SO level (only slightly better than without SO inclusion) with a maximum deviation of only 0.5 ppm downfield whereas the BP86/TZ2P/SO computed values deviate by 2 ppm upfield. For the  $^{13}\text{C}$  NMR, the maximum deviation obtained at the B3LYP/TZ2P/SO and BP86/TZ2P/SO levels are 6 ppm and 2.5 ppm downfield, respectively. Both B3LYP and BP86 methods are successful in predicting the  $^1\text{H}$  NMR values with a maximum deviation of 1.5 ppm. In the case of the tantalum cluster **3'**,  $^{11}\text{B}$  NMR chemical shifts computed at the B3LYP/TZ2P level including SO contributions result in a good agreement with the experimentally observed values with a maximum deviation of 3 ppm upfield (7 ppm at the BP86/TZ2P/SO level). We note that the inclusion of the SO term increases considerably the accuracy. The  $^{13}\text{C}$  NMR chemical shift values are computed with a maximum deviation of 3 ppm at the BP86/TZ2P/SC level and 6 ppm at the B3LYP/TZ2P/SC level. Though the inclusion of SO term has a considerable effect on  $^{11}\text{B}$  NMR chemical shifts, only a small effect (0.3 ppm) is observed for the chemical shifts of the methyl and cyclopentadienyl carbon atoms. The computed  $^1\text{H}$  NMR chemical shifts for the terminal and bridging hydrogen atoms are comparable at both B3LYP/TZ2P/SO and BP86/TZ2P/SO levels with deviations of 1-2 ppm.

When comparing compounds **1**, **2**, and **3'**, i.e., from V to Ta, the boron atoms and the bridging hydrogen atoms experience slightly more shielding but the reverse situation is observed for terminal hydrogen atoms. A look at the individual B3LYP/TZ2P/SO computed components



$\sigma_{(\text{dia})}$ ,  $\sigma_{(\text{para})}$ , and  $\sigma_{(\text{so})}$  of the shielding tensors indicates that the diamagnetic shielding largely dominates in all the cases as expected and is comparable in all clusters (Fig. 1). On the other hand, the paramagnetic shielding decreases considerably while going from V to Ta, from -105 ppm to -71 ppm. Not surprisingly, the shielding from the relativistic spin-orbit term strongly increases from -0.3 for V and Nb to -7.0 ppm for Ta. In fact, the large low-field shifts, which are characteristics of the effect of the neighboring transition metals on  $^{11}\text{B}$  NMR resonances, were already ascribed to the paramagnetic term by Fehlner et al. [34].

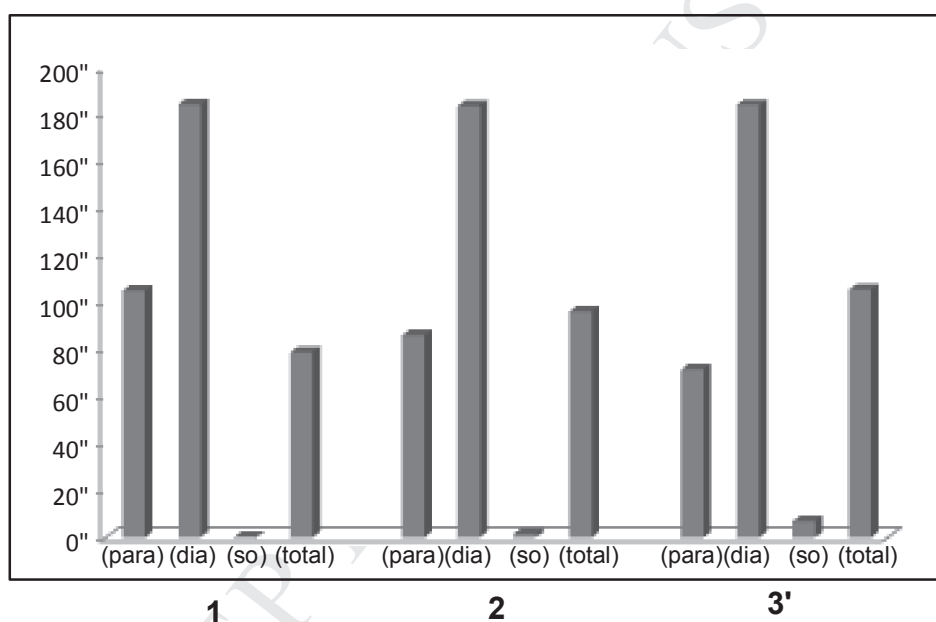


**Fig. 1.** Individual components of shielding tensors (ppm)  $\sigma_{(\text{para})}$ ,  $\sigma_{(\text{dia})}$  and  $\sigma_{(\text{so})}$  vs. total shielding in  $^{11}\text{B}$  NMR of compounds **1**, **2**, and **3'**.  $\sigma_{(\text{para})}$  and  $\sigma_{(\text{so})}$  are plotted as  $|\sigma_{(\text{para})}|$  and  $|\sigma_{(\text{so})}|$ .

For the metallaborane clusters  $(\text{Cp}^*\text{Mo})_2(\text{B}_2\text{H}_6)_2$  (**5**) and  $(\text{Cp}^*\text{W})_2(\text{B}_2\text{H}_6)_2$  (**6**), a single signal in the  $^{11}\text{B}$  NMR is also experimentally observed supporting the highly symmetric nature of these clusters in solution. For **5** a signal is observed experimentally at -58.6 ppm in the low frequency region. With the BP86 functional, deviations up to 6 ppm (without SO) or 7 ppm (with SO) in

the upfield region are calculated (Table 4). Maximum deviations of upfield 2 ppm (without SO) and 4 ppm (with SO) are computed with the B3LYP functional. More surprisingly, the  $^{11}\text{B}$  NMR signal computed for **6** compares moderately to that experimentally measured at -53.9 ppm. The closest computed value, which deviates by 10 ppm, is obtained at the B3LYP level (without SO). A good agreement between theory and experiment (0-2 ppm deviation) is observed for the  $^1\text{H}$  NMR chemical shifts of the terminal and bridging hydrogen atoms with both methods (without SO).

NMR data measured experimentally suggest that the electron-deficient cluster  $(\text{Cp}^*\text{Cr})_2\text{B}_4\text{H}_8$ , **10**, is diamagnetic [61]. Two distinct boron environments are expected from a doublet signal at 126.5 ppm and a multiplet signal at 34.3 ppm (Table 5). Interestingly, the BP86/TZ2P computed values of 15.9, 22.4, 22.2, and 16.6 ppm for B3, B4, B5, and B6, respectively, strongly differ, especially those for B4 and B5. With two hydrogen atoms more, the corresponding values change to 36.6, 32.4, 33.6, and 37.2 ppm. A good agreement with the experimental values is then observed for B3 and B6, but again not for the experimentally unusually shielded B4 and B5 atoms. These results suggest that compound **10** should probably be corrected into  $(\text{Cp}^*\text{Cr})_2\text{B}_4\text{H}_{10}$ , **12**, and that the experimental boron chemical shifts of 126.5 ppm have been wrongly attributed to B4 and B5 atoms. Concerning, the  $^1\text{H}$  NMR chemical shifts, the best agreement is observed between values experimentally measured for **10** and values theoretically computed for **12**. For comparison, the  $^{11}\text{B}$  NMR chemical shifts were computed for the cluster  $(\text{Cp}^*\text{Cr})_2\text{B}_4\text{H}_6(\text{CO})_2$  (**11**) for which the two corresponding signals are experimentally observed at 63.9 and 34.9 ppm. A good agreement is found at either at BP86 or B3LYP levels of theory (Table 5).

$^{11}\text{B}$  NMR chemical shifts of the two types of boron atoms ( $\text{B}_2$ ,  $\text{B}_3$  and  $\text{B}_4$ ) directly bonded to the metal atoms in  $(\text{Cp}^*\text{M})_2\text{B}_5\text{H}_9$  ( $\text{M} = \text{Cr}$  (**7**),  $\text{Mo}$  (**8**),  $\text{W}$  (**9**)) experience a large systematic shift to higher field going from Cr to Mo to W, whereas the shift at upper field for the boron atoms ( $\text{B}_1$ ,  $\text{B}_5$ ) connected to the metal atoms via M-H-B bridged bonds are invariant (Table ST5 (Supporting Information) and Fig. 2). This trend is also predicted by the DFT calculations, although the agreement between computed and experimental values is far to be satisfactory. For **7** the better chemical shifts are computed at the BP86/TZ2P/SC level with a deviation of 3.5 ppm for  $\text{B}_1/\text{B}_5$ , but 13 ppm for  $\text{B}_2/\text{B}_4$  and 18 ppm for  $\text{B}_3$  downfield. Except for  $\text{B}_3$  for which a deviation of 9 ppm is observed, the computed B3LYP/TZ2P/SC values differ by more than 20 ppm downfield. On the other hand, B3LYP/TZ2P/SC computed values for the Mo analogue **8** and B3LYP/TZ2P/SO computed values for the W analogue **9** are in a very good agreement with the experimental values with a maximum deviation of 3 ppm downfield (Table 4 and Fig. 2). Inclusion of relativistic spin-orbit corrections for the latter improves the B3LYP/TZ2P/SC computed  $^{11}\text{B}$  NMR chemical shifts considerably by ca. 7 ppm. Both B3LYP and BP86 computed  $^1\text{H}$  NMR  $\delta$  values for the B-H terminal and M-H-B bridging hydrogen atoms in close agreement with the experimental values with a maximum deviation of ca. 1 ppm.

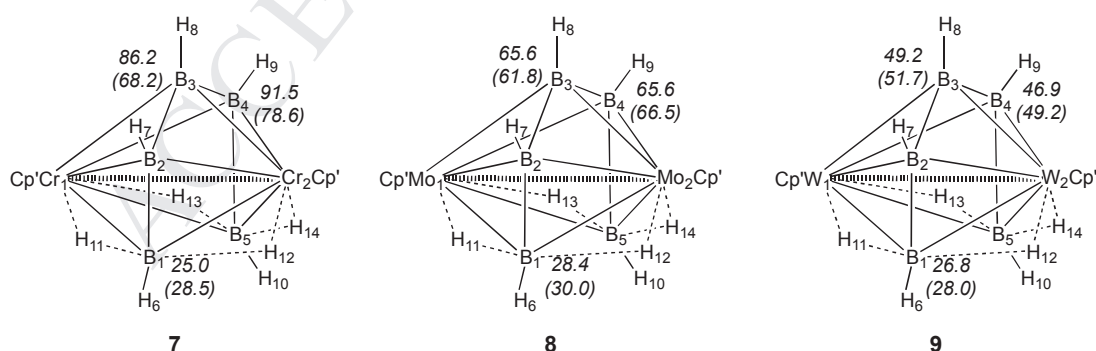


**Fig. 2.** Experimental and most accurate computed (in brackets)  $^{11}\text{B}$  NMR chemical shifts (ppm) for compounds **7-9** (BP86/TZ2P/SC for **7**, B3LYP/TZ2P/SC for **8**, and B3LYP/TZ2P/SO for **9**).

$^{11}\text{B}$  NMR chemical shifts were also computed for the late transition metal borane compounds in order to also check the suitability of the computational method used (Table ST6 and Fig. 3). Experimentally, the *nido*-2,4-(Cp\*Co) $_2\text{B}_3\text{H}_7$  compound **15** exhibits two  $^{11}\text{B}$  NMR signals in a 2:1 ratio at 65.8 ppm and -18.1 ppm [5]. Correct values (Table 10) with deviations of a few ppm are computed at the BP86/TZ2P/SC, BP86/TZ2P/SO, and B3LYP/TZ2P/SC levels (the latter is slightly better). Good values are also computed for the  $^1\text{H}$  NMR chemical shifts, especially at the B3LYP/TZ2P/SC level with maximum deviations of ca. 1 ppm. The signals of the two terminal hydrogen atoms H6 and H8, not attributed experimentally are computed to resonate around 0 ppm, justifying the possibility of overlapping experimentally with the H peak of TMS [5] and the strength of the computational methods used. For the *nido*-1,2-(Cp\*Rh) $_2\text{B}_3\text{H}_7$  species **16**, the experimental  $^{11}\text{B}$  NMR spectrum results with four broad signals at 3.1, 5.8, 8.2, and 11.1 ppm and a very broad signal at 21.1 ppm [7]. Since only three signals are expected, these five signals must be due to the presence of two tautomers (**16** and **16b** for instance, see above) or even other additional species in solution, as confirmed later with variable-temperature NMR [7]. Indeed, calculations seem to indicate a more complex situation. Although, the different levels of calculations lead to somewhat different values (up to 10 ppm difference), they show the same trend with the three boron atoms in **16** resonating in the same range around 0-10 ppm (Table 5 and Fig. 3), and the three boron atoms in **16b** resonating strongly differently around -12 (B3), 1 (B4) and 48 (B5) ppm. With no experimental peaks measured at such low or high frequencies, we might conclude that **16b** is not present in the solution of **16** and that the additional peak such as at 21 ppm are due to other species. Interestingly, the  $^{11}\text{B}$  NMR peaks for the chlorine-analogue cluster (Cp\*Rh) $_2\text{B}_3\text{H}_6\text{Cl}$  show experimental  $^{11}\text{B}$  NMR chemical shifts at 48.0, 4.0, and -5.3 ppm for the three boron atoms [11].

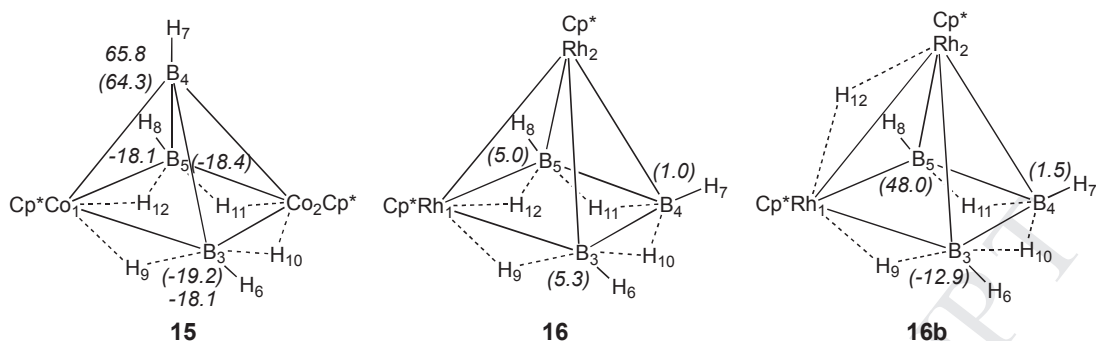


**Fig. 3.** DFT computed chemical shift values (ppm, in brackets) for clusters **15** (B3LYP/TZ2P/SC) and **16, 16b** (B3LYP/TZ2P/SO). Experimental values for **15** are given for comparison.

## Conclusion

The present study proves the strength of DFT methods in analyzing the electronic and magnetic properties of a series of dimetallaboranes with both early- and late-transition metals. In particular, the observed  $^1\text{H}$  and  $^{11}\text{B}$  chemical shifts of most of the studied compounds can be reproduced with a rather good accuracy of a few ppm at the DFT-GIAO BP86/TZ2P/SC level for the compounds with first-row transition metal elements and at the B3LYP/TZ2P/SO level for those with second- and third-row transition metal elements. This shows that the quality of DFT computed  $^1\text{H}$  and  $^{11}\text{B}$  chemical shifts generally attained for boranes and carboranes does not degrade much in the presence of transition metals, suggesting that any metallaborane is amenable to relatively accurate  $^1\text{H}$  and  $^{11}\text{B}$  NMR computations. Indeed, the accuracy is sufficient for structural applications to elucidate the number and the location of bridging hydrogen atoms in experimentally poorly characterized metallaboranes such as  $(\text{Cp}^*\text{Cr})_2\text{B}_4\text{H}_8$ .

## Acknowledgments

The authors acknowledge the Indo-French Centre for Promotion of Advanced Research (IFCPAR) (Project No. 4405-1) for generous financial support. Dr. B. Le Guennic (Rennes) is thanked for helpful discussions.

## Appendix. Supplementary data

Supplementary data (Tables ST1-ST6 and Cartesian coordinates of all optimized geometries) related to this article can be found at <http://dx.doi.org/10.1016/j.jorganchem...>

## References

- [1] T. P. Fehlner, J.-F. Halet, J.-Y. Saillard, *Molecular Clusters. A Bridge to Solid-State Chemistry*, Cambridge University Press, New York, 2007.
- [2] T. P. Fehlner, *Organometallics* 19 (2000) 2643-2651.
- [3] R. B. King, *Inorg. Chem.* 43 (2004) 4241-4247.
- [4] T. P. Fehlner, *Organometallics* 19 (2000) 2643-2651.
- [5] Y. Nishihara, K. J. Deck, M. Shang, T. P. Fehlner, B. S. Haggerty, A. L. Rheingold, *Organometallics* 13 (1994) 4510-4522.
- [6] X. Lei, M. Shang, T. P. Fehlner, *J. Am. Chem. Soc.* 120 (1998) 2686-2687.
- [7] H. Yan, A. M. Beatty, T. P. Fehlner, *Organometallics* 21 (2002) 5029-5037.
- [8] X. Lei, M. Shang, T. P. Fehlner, *Chem. Eur. J.* 6 (2000) 2653-2664.
- [9] S. Ghosh, B. C. Noll, T. P. Fehlner, *Dalton Trans.* (2008) 371-378.
- [10] K. Geetharani, S. K. Bose, G. Pramanik, T. K. Saha, V. Ramkumar, S. Ghosh, *Eur. J. Inorg. Chem.* (2009) 1483-1487.

- [11] X. Lei, M. Shang, T. P. Fehlner, *J. Am. Chem. Soc.* 121 (1999) 1275-1287.
- [12] A. S. Weller, M. Shang, T. P. Fehlner, *Chem. Commun.* (1998) 1787-1788.
- [13] B. LeGuennic, H. Jiao, S. Kahlal, J.-Y. Saillard, J.-F. Halet, S. Ghosh, M. Shang, A. M. Beatty, A. L. Rheingold, T. P. Fehlner, *J. Am. Chem. Soc.* 126 (2004) 3203-3217.
- [14] J. Ho, K. J. Deck, Y. Nishihara, M. Shang, T. P. Fehlner, *J. Am. Chem. Soc.* 117 (1995) 10292-10299.
- [15] S. Aldridge, H. Hashimoto, K. Kawamura, M. Shang, T. P. Fehlner, *Inorg. Chem.* 37 (1998) 928-940.
- [16] H. J. Bullick, P. D. Grebenik, M. L. H. Green, A. K. Hughes, J. B. Leach, P. C. McGowan, *J. Chem. Soc. Dalton Trans.* (1995) 67-75.
- [17] S. Aldridge, M. Shang, T. P. Fehlner, *J. Am. Chem. Soc.* 120 (1998) 2586-2598.
- [18] S. Sahoo, R. S. Dhayal, B. Varghese, S. Ghosh, *Organometallics* 28 (2009) 1586-1589.
- [19] A. S. Weller, M. Shang, T. P. Fehlner, *Organometallics* 18 (1999) 53-64.
- [20] S. K. Bose, S. Ghosh, B. C. Noll, J.-F. Halet, J.-Y. Saillard, A. Vega, *Organometallics* 26 (2007) 5377-5385.
- [21] C. Ting, L. Messerle, *J. Am. Chem. Soc.* 111 (1989) 3449-3450.
- [22] S. Aldridge, H. Hashimoto, M. Shang, T. P. Fehlner, *J. Chem. Soc. Chem. Commun.* (1998) 207-208.
- [23] S. K. Bose, K. Geetharani, B. Varghese, S. M. Mobin, S. Ghosh, *Chem. Eur. J.* 14 (2008) 9058-9064.
- [24] T. Onak, J. Tseng, M. Diaz, D. Tran, J. Arias, S. Herrera, D. Brown, *Inorg. Chem.* 32 (1993) 487-489.
- [25] G. Schreckenbach, T. Ziegler, *Theor. Chem. Acc.* 99 (1998) 71-82.

- [26] M. Bühl, D. Hnyk, J. Macháček, *Chem. Eur. J.* 11 (2005) 4109-4120.
- [27] M. Bühl, J. Holub, D. Hnyk, J. Macháček, *Organometallics* 25 (2006) 2173-2181.
- [28] M. Bühl, D. Hnyk, J. Macháček, *Inorg. Chem.* 46 (2007) 1771-1777.
- [29] K. Geetharani, B. S. Krishnamoorthy, S. Kahlal, S. M. Mobin, J.-F. Halet, S. Ghosh, *Inorg. Chem.* 51 (2012) 10176 - 10184.
- [30] B. S. Krishnamoorthy, A. Thakur, K. Chakrahari, S. Bose, P. Hamon, T. Roisnel, S. Kahlal, S. Ghosh, J.-F. Halet, *Inorg. Chem.* 51 (2012) 10375 - 10383.
- [31] B. S. Krishnamoorthy, S. Kahlal, S. Ghosh, J.-F. Halet, *Theor. Chem. Acc.* 132 (2013) 1356-1366.
- [32] B. S. Krishnamoorthy, S. Kahlal, B. Le Guennic, J.-Y. Saillard, S. Ghosh, J.-F. Halet *Sol. State Sci.* 14 (2012) 1617–1623.
- [33] S. K. Bose, S. M. Mobin, S. Ghosh, *J. Organomet. Chem.* 696 (2011) 3121-3126.
- [34] A. S. Weller, T. P. Fehlner, *Organometallics* 18 (1999) 447-450.
- [35] Y. Nishihara, K. J. Deck, M. Shang, T. P. Fehlner, V. A. Haggerty, L. Rheingold, *Organometallics* 13 (1994) 4510-4522.
- [36] ADF2010.02, SCM, Theoretical Chemistry, Vrije Universiteit, Amsterdam, The Netherlands, <http://www.scm.com>.
- [37] G.teVelde, F. M. Bickelhaupt, E. J. Baerends, S.J. A. van Gisbergen, C. Fonseca Guerra, J. G. Snijders, T. Ziegler, *J. Comput. Chem.* 22 (2001) 931-967.
- [38] S. H. Vosko, L. Wilk, M. Nusair, *Can. J. Phys.*, 58 (1980) 1200-1211.
- [39] A. D. Becke, *J. Chem. Phys.* 84 (1986) 4524-4529.
- [40] A. D. Becke, *Phys. Rev. A* 38 (1986) 3098-3100.



- [41] J. P. Perdew, *Phys. Rev. B* 33 (1986) 8822-8824.
- [42] L. Versluis, T. Ziegler, *J. Chem. Phys.* 88 (1988) 322-329.
- [43] E. van Lenthe, E. J. Baerends, J. G. Snijders, *J. Chem. Phys.* 99 (1993) 4597-4610.
- [44] E. van Lenthe, E. F. Baerends, J. G. Snijders, *J. Chem. Phys.* 101 (1994) 9783-9792.
- [45] E. van Lenthe, R. van Leeuwen, E. J. Baerends, J. G. Snijders, *Int. J. Quantum. Chem.* 57 (1996) 281-293.
- [46] A. D. Becke, *Phys. Rev. A*, 38 (1988) 3098-3100.
- [47] C. Lee, W. Yang, R. G. Parr, *Phys. Rev. B* 37 (1988) 785-789.
- [48] A. D. Becke, *J. Chem. Phys.*, 98 (1993) 5648-5652.
- [49] F. London, *J. Phys. Radium* 27 (1937) 397-409.
- [50] R. Ditchfield, *Mol. Phys.* 27 (1974) 789-807.
- [51] K. Wolinski, J. F. Hinton, P. Pulay, *J. Am. Chem. Soc.* 112 (1990) 8251-8260.
- [52] K. Friedrich, G. Seifert, G. Grossmann, *Z. Phys. D*, 17 (1990) 45-46.
- [53] G Schreckenbach, T. Ziegler, *J. Phys. Chem.* 99 (1995) 606-611.
- [54] G. Schreckenbach, T. Ziegler, *Int. J. Quantum. Chem.* 61 (1997) 899-918.
- [55] G. Schreckenbach, T. Ziegler, *Int. J. Quantum. Chem.* 60 (1996) 753-766.
- [56] S. K. Wolff, T. Ziegler, *J. Chem. Phys.* 109 (1998) 895-905.
- [57] S. K. Wolff, T. Ziegler, E. van Lenthe, E. J. Baerends, *J. Chem. Phys.* 110 (1999) 7689-7698.
- [58] T. P. Fehner, *Collect. Czech. Chem. Commun.* 64 (1999) 767-782.

- [59] S. K. Bose, K. Geetharani, V. Ramkumar, S. M. Mobin, S. Ghosh, *Chem. Eur. J.* 15 (2009) 13483-13490.
- [60] J. Emsley, *The Elements*, Oxford University Press, Oxford, 3rd Ed., 1998.
- [61] K. J. Deck, Y. Nishihara, M. Shang, T. P. Fehlner, *J. Am. Chem. Soc.* 116 (1994) 8408-8409.
- [62] S. K. Bose, S. Ghosh, B. C. Noll, J.-F. Halet, J.-Y. Saillard, A. Vega, *Organometallics* 26 (2007) 5377-5385.
- [63] S. Ghosh, M. Shang, T. P. Fehlner, *J. Organomet. Chem.*, 614-615 (2000) 92-98.
- [64] M. David Curtis, W. M. Butler, *J. Organomet. Chem.* 155 (1978) 131-145.
- [65] K. Wade, *J. Chem. Soc. D.* (1971) 792-793.
- [66] K. Wade, *Adv. Inorg. Chem. Radiochem.* 18 (1976) 1-66.
- [67] K. Wade, in *Transition Metal Clusters*, B. F. G. Johnson (ed.), Wiley, Chichester, 1980, pp. 193–264.
- [68] D.M.P. Mingos, *Nature Phys. Sci.* 236 (1972) 99-102.
- [69] D. M. P. Mingos, *Acc. Chem. Res.* 17 (1984) 311-319.
- [70] D. M. P. Mingos, D. J. Wales, *Introduction to Cluster Chemistry*, Prentice-Hall, Englewood Cliffs, 1990.
- [71] R. B. King, *Inorg. Chem.* 45 (2006) 8211-8216.
- [72] R. B. King, S. Ghosh, *Theor. Chem. Acc.* 131 (2012) 1087.

- [73] J.-F. Halet, J.-Y. Saillard, in: J. Reedijk, K. Poeppelmeier (eds.), *Comprehensive Inorganic Chemistry II*, Elsevier, Oxford, 2013 vol. 9: Theory and Methods (S. Alvarez, volume ed.), p. 869-885.
- [74] D. M. Hoffman, R. Hoffmann, C. R. Fisel, *J. Am. Chem. Soc.* 104 (1982) 3858-3875.
- [75] J. Autschbach, T. Ziegler, in: *Encyclopedia of Nuclear Magnetic Resonance*, Vol. 9, *Advances in NMR*, John Wiley and Sons, Chichester, 2002, pp. 306-323.

**Table 1**

Selected bond parameters (Å) for the compounds (CpM)<sub>2</sub>(B<sub>2</sub>H<sub>6</sub>)<sub>2</sub> (**1** M = V; **2** M = Nb; **3** M = Ta) and (Cp\*M)<sub>2</sub>(B<sub>2</sub>H<sub>6</sub>)<sub>2</sub> (**1'** M = V; **2'** M = Nb; **3'** M = Ta; **4** M = Cr; **5** M = Mo; **6** M = W) (Cp = η<sup>5</sup>-C<sub>5</sub>H<sub>5</sub>; Cp\* = η<sup>5</sup>-C<sub>5</sub>Me<sub>5</sub>) optimized at the BP86/TZ2P all-electron ZORA level and corresponding experimental X-ray values [59] where available.

Cmpd.	<b>1</b>	<b>1'</b>	<b>2</b>	<b>2</b>	<b>2'</b>	<b>3</b>	<b>3'</b>	<b>3'</b>	<b>3'</b>	<b>4</b>	<b>5</b>	<b>6</b>
	Exp.	BP86/ TZ2P/ SC	BP86/ TZ2P/SC	Exp.	BP86/ TZ2P/SC	BP86/ TZ2P/SC	Exp.	BP86/ TZ2P/SC	BP86/ TZ2P/SC	BP86/ TZ2P/SC	BP86/ TZ2P/SC	BP86/ TZ2P/SC
M1-M2	2.787(2)	2.735	2.735	2.948(16)	2.954	2.943	2.933(4)	2.941	2.760	2.900	2.909	
M1-B3	2.295(7)	2.269	2.271	2.410(12)	2.405	2.385	2.387(13)	2.386	2.291	2.414	2.395	
M1-B4	2.301(6)	2.269	2.273	2.421(11)	2.404	2.384	2.363(15)	2.385	2.291	2.413	2.398	
M1-B5	2.285(6)	2.269	2.273	2.421(11)	2.404	2.387	2.369(15)	2.387	2.291	2.414	2.407	
M1-B6	2.284(5)	2.27	2.271	2.410(12)	2.405	2.388	2.374(12)	2.388	2.292	2.414	2.406	
M2-B3	2.285(6)	2.269	2.273	2.414(11)	2.404	2.387	2.369(15)	2.387	2.291	2.413	2.407	
M2-B4	2.284(5)	2.27	2.271	2.422(11)	2.405	2.388	2.374(12)	2.388	2.292	2.414	2.406	
M2-B5	2.295(7)	2.269	2.271	2.422(11)	2.405	2.385	2.387(13)	2.386	2.291	2.414	2.395	
M2-B6	2.301(6)	2.269	2.273	2.414(11)	2.404	2.384	2.363(15)	2.385	2.291	2.414	2.398	
B3-B4	1.734(7)	1.752	1.750	1.819(19)	1.785	1.773	1.751(3)	1.772	1.671	1.690	1.686	
B5-B6	1.734(7)	1.752	1.750	1.819(19)	1.785	1.773	1.751(3)	1.772	1.671	1.690	1.686	

**Table 2**

Selected bond parameters (Å) for the compounds (Cp\*Cr)<sub>2</sub>B<sub>4</sub>H<sub>8</sub> (**10**), (Cp\*Cr(CO))<sub>2</sub>B<sub>4</sub>H<sub>6</sub> (**11**) and (Cp\*Cr)<sub>2</sub>B<sub>4</sub>H<sub>10</sub> (**12**) optimized at the BP86/TZ2P all electron ZORA level with corresponding experimental X-ray values where available.

Compound	<b>10</b>		<b>11</b>		<b>12</b>	
	Exp.	BP86/TZ2P/SC	Exp.	BP86/TZ2P/S	Exp.	BP86/TZ2P/SC
Cr1-Cr2	2.870(2)	2.548	2.792(1)	2.764	2.736	2.736
Cr1-B3	2.13(2)	2.18	2.16(1)	2.189	2.196	2.196
Cr1-B4	2.01(2)	2.171	2.13(1)	2.171	2.164	2.164
Cr1-B5	2.01(2)	2.17	2.11(1)	2.148	2.164	2.164
Cr1-B6	2.11(2)	2.178	2.17(1)	2.169	2.190	2.190
Cr2-B3	2.15(2)	2.18	2.16(1)	2.170	2.194	2.194
Cr2-B4	2.02(1)	2.173	2.13(1)	2.149	2.162	2.162
Cr2-B5	2.04(2)	2.172	2.11(1)	2.171	2.161	2.161
Cr2-B6	2.12(2)	2.180	2.17(1)	2.189	2.196	2.196
B3-B4	1.75(3)	1.735	1.66(2)	1.701	1.701	1.701
B4-B5	1.75(3)	1.637	1.63(2)	1.652	1.639	1.639
B5-B6	1.61(3)	1.735	1.66(2)	1.702	1.702	1.702

**Table 3**

DFT BP86/TZ2P and B3LYP/TZ2P computed (scalar/spin orbit ZORA) and experimental NMR chemical shifts  $\delta$  (ppm) for the compounds  $(\text{CpM})_2(\text{B}_2\text{H}_6)_2$  (**1** M = V Cp =  $\text{C}_5\text{H}_5$ ; **2** M = Nb, Cp =  $\text{C}_5\text{H}_5$ ; **3** M = Ta, Cp =  $\text{C}_5\text{Me}_5$ ).

Compound	<b>1</b>					<b>2</b>					<b>3'</b>				
	Exp.	BP86/ TZ2P/S C	BP86/ TZ2P/ SO	B3LYP /TZ2P/ SC	B3LYP SO	Exp.	BP86/ TZ2P/ SC	BP86/ TZ2P/ SO	B3LYP/T Z2P/SC	B3LYP/ TZ2P/ SO	Exp.	BP86/ TZ2P/ SC	BP86/ TZ2P/ SO	B3LYP/T Z2P/SC	B3LYP/ TZ2P/ SO
<i><sup>11</sup>B NMR</i>															
B3	1.7	5.6	5.9	19.2	19.5	1.7	-6.1	-4.1	0.6	2.2	-4.0	-18.9	-11.2	-13.9	-7.0
B4	1.7	5.6	5.9	19.2	19.5	1.7	-6.1	-4.1	0.6	2.2	-4.0	-18.9	-11.3	-13.9	-7.1
B5	1.7	5.6	5.9	19.2	19.5	1.7	-6.1	-4.1	0.6	2.2	-4.0	18.9	-11.2	-13.9	-7.0
B6	1.7	5.6	5.9	19.2	19.5	1.7	-6.1	-4.1	0.6	2.2	-4.0	18.9	-11.3	-13.9	-7.1
<i><sup>1</sup>H NMR</i>															
H9	3.4	2.7	3.1	3.0	3.5	4.1	2.4	3.3	2.5	3.3	4.4	1.6	3.7	1.7	3.4
H10	3.4	2.7	3.1	3.0	3.5	4.1	2.4	3.2	2.5	3.3	4.4	1.6	3.7	1.7	3.4
H15	3.4	2.7	3.1	3.0	3.5	4.1	2.4	3.2	2.5	3.3	4.4	1.6	3.7	1.7	3.4
H16	3.4	2.7	3.1	3.0	3.5	4.1	2.4	3.3	2.5	3.3	4.4	1.6	3.7	1.7	3.4
H12	-9.7	-10.3	-10.5	-10.8	-11.1	-10.1	-10.0	-10.8	-10.3	-10.9	-10.5	-10.2	-12.5	-10.5	-11.7
H8	-9.7	-9.9	-10.1	-10.4	-10.6	-10.1	-9.8	-10.4	-10.0	-10.6	-10.5	-10.2	-12.5	-10.5	-11.6
H13	-9.7	-9.9	-10.1	-10.4	-10.6	-10.1	-9.8	-10.4	-10.0	-10.6	-10.5	-10.6	-12.8	-10.8	-11.8
H17	-9.7	-10.3	-10.5	-10.8	-11.1	-10.1	-10.0	-10.8	-10.3	-10.9	-10.5	-10.6	-12.8	-10.8	-11.9
H7	-9.7	-9.9	-10.1	-10.4	-10.6	-10.1	-9.8	-10.5	-10.1	-10.5	-10.5	-10.6	-12.8	-10.8	-11.8
H11	-9.7	-10.3	-10.5	-10.8	-11.1	-10.1	-10.0	-10.5	-10.3	-10.7	-10.5	-10.6	-12.8	-10.8	-11.9
H18	-9.7	-10.3	-10.5	-10.8	-11.1	-10.1	-10.0	-10.5	-10.3	-10.7	-10.5	-10.2	-12.5	-10.5	-11.7
H14	-9.7	-9.9	-10.1	-10.4	-10.6	-10.1	-9.8	-10.5	-10.1	-10.5	-10.5	-10.2	-12.5	-10.5	-11.6

CpH	5.4	5.4	5.3	5.4	5.4	5.4	5.4	5.7	6.0	6.0	5.9	6.0	2.26	2.0	2.2	2.0	2.1
$^{13}\text{C NMR}$																	
C <sub>Cp</sub>	97.8	91.6	91.5	95.1	95.1	95.1	97.2	99.7	99.6	102.6	103.6	109.6	113.4	113.3	116.9	116.5	
C <sub>Me</sub>	-	-	-	-	-	-	-	-	-	-	-	13.5	10.3	10.8	10.6	11.3	

**Table 4**

DFT BP86/TZ2P and B3LYP/TZ2P computed (scalar/spin orbit ZORA) and experimental NMR chemical shifts  $\delta$  (ppm) for the compounds  $(\text{Cp}^*\text{M})_2(\text{B}_2\text{H}_6)_2$  (**4** M = Cr; **5** M = Mo; **6** M = W).

Cmpd.	4					5					6				
	BP86/ TZ2P/ SC	BP86/ TZ2P/ SO	B3LYP/ /TZ2P/ SC	B3LYP/ TZ2P/SO	Exp.	BP86/ TZ2P/ SC	BP86/ TZ2P/ SO	B3LYP/ TZ2P/SC	B3LYP/ TZ2P/SO	Exp.	BP86/ TZ2P/ SC	BP86/T Z2P/SO	B3LYP/ TZ2P/SC	B3LYP/ TZ2P/SO	Exp.
$^{11}\text{B}$ NMR															
B3	-65.5	-66.9	-61.2	-62.9	-58.6	-64.2	-65.8	-60.5	-62.8	-53.9	-68.2	-70.7	-63.7	-67.5	-53.9
B4	-65.7	-67.1	-61.3	-63.1	-58.6	-64.3	-65.8	-60.7	-63.0	-53.9	-68.5	-71.2	-64.0	-67.9	-53.9
B5	-65.5	-66.9	-61.2	-62.9	-58.6	-64.2	-65.7	-60.6	-62.9	-53.9	-68.2	-70.7	-63.7	-67.5	-53.9
B6	-65.7	-67.1	-61.3	-63.1	-58.6	-64.0	-65.6	-60.4	-62.6	-53.9	-68.5	-71.2	-64.0	-67.9	-53.9
$^1\text{H}$ NMR															
H9	-0.8	-0.8	-1.2	-2.0	0.6	-0.1	-1.4	-0.2	-1.5	0.3	-0.2	-3.0	-0.3	-3.2	0.3
H10	-0.9	-0.9	-1.2	-2.0	0.6	-0.2	-1.3	-0.2	-1.5	0.3	-0.2	-3.0	-0.3	-3.2	0.3
H15	-0.8	-0.8	-1.2	-2.0	0.6	-0.1	-1.3	-0.2	-1.5	0.3	-0.2	-3.0	-0.3	-3.2	0.3
H16	-0.9	-0.9	-1.2	-2.0	0.6	-0.1	-1.3	-0.1	-1.4	0.3	-0.2	-3.0	-0.3	-3.2	0.3
H12	-14.8	-16.0	-16.6	-18.0	-12.4	-10.7	-12.5	-11.3	-13.2	-10.2	-9.4	-15.0	-9.8	-14.6	-10.2
H8	-14.2	-15.4	-16.1	-17.5	-12.4	-10.4	-12.6	-11.1	-13.0	-10.2	-9.6	-15.3	-10.1	-14.9	-10.2
H13	-14.2	-15.4	-16.1	-17.5	-12.4	-10.3	-12.5	-11.1	-13.0	-10.2	-10.4	-16.1	-10.7	-15.4	-10.2
H17	-14.9	-16.1	-16.5	-17.9	-12.4	-10.6	-12.6	-11.3	-13.1	-10.2	-10.0	-15.7	-10.4	-15.1	-10.2
H7	-14.2	-15.4	-16.1	-17.5	-12.4	-10.4	-12.5	-11.1	-13.1	-10.2	-10.4	-16.1	-10.7	-15.4	-10.2
H11	-14.9	-16.1	-16.5	-17.9	-12.4	-10.7	-13.1	-11.3	-13.3	-10.2	-10.0	-15.7	-10.4	-15.1	-10.2
H18	-14.8	-16.0	-16.6	-18.0	-12.4	-10.6	-13.0	-11.2	-13.3	-10.2	-9.4	-15.0	-9.8	-14.6	-10.2
H14	-14.2	-15.4	-16.1	-17.5	-12.4	-10.34	-12.5	-11	-13.0	-10.2	-9.6	-15.3	-10.1	-14.9	-10.2



CpH	0.6	0.7	0.7	0.7	1.4	1.4	1.4	1.4	1.44	1.7	1.5	1.7	1.5	1.7	1.7
$^{13}\text{C}$ NMR															
C <sub>Me</sub>					8.5	8.4	8.9	9.0			8.8	9.8	9.4	10.7	
C <sub>Cp</sub>		108.3	108.1	108.1	108.7	108.4	111.8	111.5		103.3	103.6	106.1	106.1	106.0	

**Table 5**

DFT BP86/TZ2P and B3LYP/TZ2P computed (scalar/spin orbit ZORA) and experimental NMR chemical shifts  $\delta$  (ppm) for the compounds  $(\text{Cp}^*\text{Cr})_2\text{B}_4\text{H}_8$  (**10**),  $(\text{Cp}^*\text{Cr})_2\text{B}_4\text{H}_6(\text{CO})_2$  (**11**), and  $(\text{Cp}^*\text{Cr})_2\text{B}_4\text{H}_{10}$  (**12**).

Cmpd.	<b>10</b>				<b>11</b>				<b>12</b>							
	Exp.	BP8 6/TZ 2P/S	BP86/TZ2 P/SO	B3LYP/ TZ2P/SC Z2P/SO	Exp.	BP86/T Z2P/SC	BP86/T Z2P/SO	B3LYP/ TZ2P/ SC	B3LYP/ 2P/SO	BP86/T Z2P/SC	BP86/TZ 2P/SO	B3LYP/ TZ2P/SC	B3LYP/ TZ2P/S O			
B3	34.3	15.9	16.7	22.5	19.5	B3	63.9	59.4	60.6	74.5	75.1	B3	36.6	36.3	46.2	46.0
B4	126.5	22.4	21.6	-18.0	-25.0	B4	34.9	22.6	22.9	34.0	33.9	B4	32.4	31.9	53.1	53.1
B5	126.5	22.2	21.5	-18.7	-22.7	B5	34.9	22.5	21.8	33.4	33.2	B5	33.6	33.7	54.7	54.8
B6	34.3	16.6	16.5	22.5	19.4	B6	63.9	59.0	58.4	73.5	73.4	B6	37.2	38.0	47.2	47.5
H7	8.5	5.8	5.8	8.0	8.5	H7	5.2	5.0	5.5	5.0	5.5	H7	4.2	4.6	3.8	4.4
H8	3.3	2.1	1.6	-0.1	-6.9	H8	2.5	2.2	2.2	2.4	2.1	H8	3.5	3.5	4.3	4.3
H9	3.3	2.1	1.7	0.0	-6.0	H9	2.5	2.2	1.9	2.5	2.3	H9	3.5	3.4	4.6	4.5
H10	8.5	5.8	5.6	8.1	8.6	H10	5.2	5.0	5.1	5.5	5.9	H10	4.1	4.3	4.0	4.5
H11	-3.9	-8.2	-9.1	-31.6	-40.8	H11	-12.7	-12.8	-12.9	-15.1	-15.4	H11	-12.4	-12.3	-14.5	-14.6
H12	-3.9	-10.4	-11.4	-38.9	-47.0	H12	-12.7	-12.8	-14.3	-15.2	-16.3	H12	-13.2	-13.1	-15.5	-15.6
H13	-3.9	-9.7	-11.6	-37.3	-45.8	H <sub>Cp</sub>	1.8	1.3	1.3	1.6	1.6	H13	-13.1	-14.7	-15.4	-16.6
H14	-3.9	-8.7	-10.5	-32.8	-42.6	C <sub>Me</sub>	104.6	107.8	107.9	108.1	108.2	H14	-12.5	-14.0	-14.7	-15.7
H <sub>Cp</sub>	1.94	1.0	1.1	0.8	1.1	C <sub>Cp</sub>	9.5	10.4	10.4	10.2	10.4	H15	-0.2	-0.7	2.8	3.0
C <sub>Me</sub>	108.7	101.2	101.1	104.3	103.5	C <sub>CO</sub>	237.1	226.4	224.6	245.5	243.0	H16	-0.7	-1.3	2.4	2.6
C <sub>Cp</sub>	12.4	7.9	7.9	6.2	4.6	C <sub>CO</sub>	237.1	226.2	224.4	246.0	243.5	H <sub>Cp</sub>	1.3	1.3	0.8	0.8
												C <sub>Me</sub>	105.7	105.6	105.7	105.7
												C <sub>Cp</sub>	10.4	10.4	11.1	11.4

# Structural, electronic and magnetic properties of some early vs late transition dimetallaborane clusters - A theoretical investigation

Kandasamy Bharathi<sup>a</sup>, Lalshab Beerma<sup>a</sup>, Chinnasamy Santhi<sup>a</sup>, Bellie Sundaram Krishnamoorthy<sup>a,b,\*</sup> and Jean-François Halet<sup>b,\*</sup>

<sup>a</sup>*Department of Chemistry, Vivekanandha College of Arts and Sciences for Women (Autonomous), Elayampalayam, Tiruchengode, 600 036, India*

<sup>b</sup>*Institut des Sciences Chimiques de Rennes, UMR 6226 CNRS-Université de Rennes 1, Avenue du Général Leclerc, 35042 Rennes Cédex, France*

## Highlights

□ The strength of DFT methods in analyzing the electronic and magnetic properties of a series of dimetallaboranes is demonstrated □ <sup>11</sup>B chemical shifts are well reproduced at the DFT-GIAO BP86/TZ2P level for first-row transition metal compounds □ B3LYP/TZ2P/SO level is necessary for second- and third-row transition metal compounds

## Supplementary material

## Structural, electronic and magnetic properties of some early vs late transition dimetallaborane clusters - A theoretical investigation

Kandasamy Bharathi<sup>a</sup>, Lalshab Beerma<sup>a</sup>, Chinnasamy Santhi<sup>a</sup>, Bellie Sundaram Krishnamoorthy<sup>a,b,\*</sup> and Jean-François Halet<sup>b,\*</sup>

<sup>a</sup>*Department of Chemistry, Vivekanandha College of Arts and Sciences for Women (Autonomous), Elayampalayam, Tiruchengode, 600 036, India*

<sup>b</sup>*Institut des Sciences Chimiques de Rennes, UMR 6226 CNRS-Université de Rennes 1, Avenue du Général Leclerc, 35042 Rennes Cédex, France*

### Table S11

Selected bond (Å) and angle (°) parameters for the compounds (Cp<sup>\*</sup>M)<sub>2</sub>B<sub>5</sub>H<sub>9</sub> (7 M = Cr; 8 M = Mo; 9 M = W) optimized at the BP86/TZ2P all-electron ZORA level with corresponding experimental X-ray values.

Compound	7		8		9	
	Exp.	BP86/TZ2P/SC	Exp.	BP86/TZ2P/SC	Exp.	BP86/TZ2P/SC
M15-M16	2.625(9)	2.592	2.809(6)	2.810	2.817(8)	2.835
M15-B1	2.193(7)	2.202	2.320(4)	2.327	2.270(2)	2.322

M15-B2	2.119(6)	2.124	2.214(4)	2.231	2.220(2)	2.240
M15-B3	2.110(5)	2.113	2.181(4)	2.213	2.170(2)	2.213
M15-B4	2.120(5)	2.124	2.209(4)	2.230	2.200(2)	2.238
M15-B5	2.206(6)	2.204	2.322(4)	2.326	2.300(2)	2.321
M16-B1	2.200(5)	2.203	2.322(4)	2.327	2.290(2)	2.322
M16-B2	2.106(5)	2.124	2.211(4)	2.234	2.220(2)	2.240
M16-B3	2.108(5)	2.114	2.176(4)	2.210	2.170(2)	2.213
M16-B4	2.107(5)	2.124	2.216(4)	2.232	2.230(2)	2.238
M16-B5	2.200(6)	2.203	2.312(4)	2.325	2.317(14)	2.321
B1-B2	1.696(10)	1.720	1.732(6)	1.758	1.700(3)	1.746
B2-B3	1.669(9)	1.681	1.715(6)	1.722	1.730(2)	1.721
B3-B4	1.661(9)	1.681	1.712(7)	1.723	1.680(2)	1.721
B4-B5	1.665(11)	1.719	1.735(7)	1.759	1.730(2)	1.746
B-B <sub>(average)</sub>	1.673	1.700	1.724	1.741	1.710	1.734
M-B <sub>(average)</sub>	2.147	2.154	2.248	2.266	2.239	2.267

**Table ST2**

Selected bond parameters ( $\text{\AA}$ ,  $^\circ$ ) for the compounds  $(\text{Cp}^*\text{Cr})_2\text{B}_4\text{H}_8$  (**10**),  $(\text{Cp}^*\text{Cr}(\text{CO}))_2\text{B}_4\text{H}_6$  (**11**) and  $(\text{Cp}^*\text{Cr})_2\text{B}_4\text{H}_{10}$  (**12**) optimized at the BP86/TZ2P all electron ZORA level with corresponding experimental X-ray values where available.

Compound	<b>10</b>		<b>11</b>		<b>12</b>	
	Exp.	BP86/TZ2P/SC	Exp.	BP86/TZ2P/S C	BP86/TZ2P/S	BP86/TZ2P/SC
Cr1-H13	na	1.682	na	1.685 <sup>a</sup>	1.667	1.667
Cr1-H12	na	1.678	na	1.685 <sup>b</sup>	1.662	1.662
Cr2-H14	na	1.683	-	-	1.661	1.661
Cr2-H11	na	1.686	-	-	1.664	1.664
B3-H13	na	1.294	na	1.321 <sup>c</sup>	1.331	1.331
B6-H12	na	1.296	na	1.321	1.334	1.334
B3-H14	na	1.292	-	-	1.335	1.335
B6-H11	na	1.292	-	-	1.333	1.333
B3-H7	na	1.207	na	1.202	1.208	1.208
B4-H8	na	1.206	na	1.202	1.206	1.206
B5-H9	na	1.206	na	1.204	1.207	1.207
B6-H10	na	1.208	na	1.202	1.208	1.208
Cr-C/H	-	-	1.817(8)	1.8432	1.5854	1.5854

Cr-C/H	na	na	na	1.843	1.5794
B3-B4-B5	111(1)	123.1	120.3(8)	120.28	121.8
B4-B5-B6	113(1)	123.1	-	120.31	121.78

<sup>a</sup> Cr1-H11. <sup>b</sup> Cr2-H12. <sup>c</sup> B3-H11. na = not available.

**Table S13**

Selected bond parameters (Å) for the compounds (Cp\*M)<sub>2</sub>B<sub>3</sub>H<sub>7</sub> (**15** M = Co; **16** and **16b** M = Rh; **17** M = Ir) optimized at the BP86/TZ2P all-electron scalar ZORA level with corresponding experimental X-ray values where available.

Compd	<b>15</b>		<b>16</b>		<b>17</b>	<b>16b</b>	
	Exp.	BP86/TZ2P/ SC	Exp.	BP86/TZ2P/SC	BP86/TZ2P/ SC	BP86/TZ2P/S C	
Co11-B1	-	2.137	M1-M2	2.74	2.773	Rh1-Rh2	2.744
Co11-B2	-	2.022	M1-B3	2.342	2.311	Rh1-B3	2.375
Co11-B3	1.986(5)	2.136	M1-B5	2.333	2.304	Rh1-B5	2.096
Co12-B1	-	2.138	B3-B4	1.827	1.858	B3-B4	1.822
Co12-B2	1.980(5)	2.022	B4-B5	1.829	1.861	B4-B5	1.826

Co12-B3	-	2.136	B3-H6	1.324(4)	1.210	1.204	B3-H6	1.207
B1-B2	1.733(8)	1.754	B4-H7	1.105(3)	1.202	1.202	B4-H7	1.203
B2-B3	1.674(9)	1.752	B5-H8	1.096(4)	1.210	1.204	B5-H8	1.201
B1-H4	1.05(7)	1.210	M1-H9	1.7905(2)	1.691	1.672	Rh1-H9	1.729
B2-H5	0.97(4)	1.207	B3-H9	1.135(3)	1.351	1.429	B3-H9	1.315
B3-H6	1.19(6)	1.210	B3-H10	1.465(3)	1.372	1.382	B3-H10	1.359
B1-H7	1.27(5)	1.319	B4-H10	1.318(4)	1.32	1.324	B4-H10	1.322
Co11-H7	1.37(5)	1.644	B4-H11	1.270(4)	1.317	1.318	B4-H11	1.299
B1-H9	1.42(5)	1.318	B5-H11	1.256(3)	1.375	1.391	B5-H11	1.397
Co12-H9	1.50(5)	1.645	B5-H12	1.345(3)	1.353	1.431	Rh2-H12	1.754
B3-H8	1.29(4)	1.320	M1-H12	1.7239(2)	1.691	1.672	Rh1-H12	1.710
Co11-H8	1.67(5)	1.642	M2-B3	2.062(3)	2.098	2.096	Rh2-B3	2.133
B3-H10	1.18(5)	1.320	M2-B4	2.061(4)	2.082	2.091	Rh2-B4	2.117
Co12-H10	1.54(5)	1.642	M2-B5	2.075(4)	2.095	2.088	Rh2-B5	2.110

---



**Table ST4**

DFT calculated (BP86/TZ2P all electron scalar ZORA level) energies of the HOMO and LUMO (eV) and HOMO-LUMO gaps ( $\Delta E$ , eV) for the complexes **1-17**.

Compound	Energy (eV)	$E_{\text{(LUMO)}}$ (eV)	$E_{\text{(HOMO)}}$ (eV)	$\Delta E$ (eV)
(CpV) <sub>2</sub> (B <sub>2</sub> H <sub>6</sub> ) <sub>2</sub> ( <b>1</b> )	-209.9264	-3.075	-4.651	1.576
(CpNb) <sub>2</sub> (B <sub>2</sub> H <sub>6</sub> ) <sub>2</sub> ( <b>2</b> )	-213.3141	-2.677	-4.441	1.764
(CpTa) <sub>2</sub> (B <sub>2</sub> H <sub>6</sub> ) <sub>2</sub> ( <b>3</b> )	-212.0582	-2.528	-4.424	1.896
(Cp*V) <sub>2</sub> (B <sub>2</sub> H <sub>6</sub> ) <sub>2</sub> ( <b>1'</b> )	-373.8117	-2.570	-4.096	1.526
(Cp*Nb) <sub>2</sub> (B <sub>2</sub> H <sub>6</sub> ) <sub>2</sub> ( <b>2'</b> )	-377.0392	-2.199	-3.91	1.711
(Cp*Ta) <sub>2</sub> (B <sub>2</sub> H <sub>6</sub> ) <sub>2</sub> ( <b>3'</b> )	-375.7596	-2.096	-3.964	1.868
(Cp*Cr) <sub>2</sub> (B <sub>2</sub> H <sub>6</sub> ) <sub>2</sub> ( <b>4</b> )	-373.6802	-2.366	-3.072	0.706
(Cp*Mo) <sub>2</sub> (B <sub>2</sub> H <sub>6</sub> ) <sub>2</sub> ( <b>5</b> )	-376.0322	-1.529	-2.944	1.415
(Cp*W) <sub>2</sub> (B <sub>2</sub> H <sub>6</sub> ) <sub>2</sub> ( <b>6</b> )	-376.0691	-1.470	-2.976	1.506
(Cp*Cr) <sub>2</sub> B <sub>3</sub> H <sub>9</sub> ( <b>7</b> )	-370.646	-2.688	-4.674	1.986
(Cp*Mo) <sub>2</sub> B <sub>5</sub> H <sub>9</sub> ( <b>8</b> )	-372.9805	-2.248	-4.661	2.413
(Cp*W) <sub>2</sub> B <sub>5</sub> H <sub>9</sub> ( <b>9</b> )	-373.2871	-2.158	-4.733	2.575
(Cp*Cr) <sub>2</sub> B <sub>4</sub> H <sub>8</sub> ( <b>10</b> )	-359.0791	-2.613	-3.259	0.646
(Cp*Cr(CO)) <sub>2</sub> B <sub>4</sub> H <sub>6</sub> ( <b>11</b> )	-384.4594	-2.658	-4.292	1.634

(Cp*Cr) <sub>2</sub> B <sub>4</sub> H <sub>10</sub> ( <b>12</b> )	-366.6190	-2.389	-4.599	2.210
(Cp*Cr) <sub>2</sub> B <sub>4</sub> H <sub>10</sub> ( <b>13</b> )	-359.3630	-2.539	-4.110	1.571
(Cp*Cr) <sub>2</sub> (B <sub>2</sub> H <sub>4</sub> ) <sub>2</sub> ( <b>14</b> )	-358.7050	-3.308	-4.286	0.978
(Cp*Co) <sub>2</sub> B <sub>3</sub> H <sub>7</sub> ( <b>15</b> )	-346.7935	-2.411	-3.569	1.158
(Cp*Rh) <sub>2</sub> B <sub>3</sub> H <sub>7</sub> ( <b>16</b> )	-344.4439	-1.958	-3.965	2.007
(Cp*Rh) <sub>2</sub> B <sub>3</sub> H <sub>7</sub> ( <b>16b</b> )	-344.4327	-1.982	-3.846	1.864
(Cp*Ir) <sub>2</sub> B <sub>3</sub> H <sub>7</sub> ( <b>17</b> )	-347.6643	-1.337	-3.951	2.614

---

Table S15

DFT BP86/TZ2P and B3LYP/TZ2P computed (Scalar/spin orbit ZORA) and experimental NMR chemical shifts  $\delta$  (ppm) for the compounds (Cp\**M*)B<sub>3</sub>H<sub>9</sub> (7 *M* = Cr; 8 *M* = Mo; 9 *M* = W).

	7				8				9						
	BP86/ TZ2P/ SC	BP86/T Z2P/SO	B3LY P/ TZ2P/ SC	B3LYP/T Z2P/ SO	Exp. TZ2P/ SC	BP86/ TZ2P/ SC	BP86/ TZ2P/ SC	B3LYP /TZ2P/ SC	B3LYP/T Z2P/ SO	Exp. TZ2P/ SC	BP86/ TZ2P/ SC	BP86/ TZ2P/ SC	B3LYP/ TZ2P/SC	B3LYP/T Z2P/ SO	
<i><sup>11</sup>B NMR</i>															
B1	25.0	28.5	28.7	46.4	46.2	28.4	21.3	23.0	30.0	31.3	26.8	15.0	22.0	21.84	28.0
B2	91.5	78.6	77.8	116.4	116.2	65.6	50.6	52.7	66.5	67.9	46.9	31.8	38.6	43.73	49.2
B3	86.2	68.2	67.5	95.2	94.9	65.6	47.9	49.3	61.8	62.8	49.2	35.8	42.1	46.98	51.7
B4	91.5	78.4	78.8	116.3	116.3	65.6	51.1	52.6	67.2	68.6	46.9	32.3	39.1	44.17	49.6
B5	25.0	28.4	29.1	47.2	47.1	28.4	21.6	23.0	30.2	31.6	26.8	15.0	22.0	21.86	28.0
<i><sup>1</sup>H NMR</i>															
H6	4.6	4.3	4.5	5.1	5.4	5.01	3.9	5.5	4.2	4.7	6.42	3.6	5.3	3.71	5.4
H7	6.7	5.2	5.5	7.1	7.6	5.61	4.0	5.0	4.5	5.5	6.42	3.0	5.4	3.33	5.7
H8	3.2	3.14	3.2	3.8	3.9	3.43	2.4	2.9	2.5	3.0	3.94	1.7	3.2	1.82	3.2
H9	6.7	5.2	5.6	6.8	7.4	5.61	4.1	5.0	4.6	5.6	6.42	3.0	5.4	3.31	5.7

H10	4.6	4.3	4.7	5.1	5.4	5.01	3.8	4.5	4.1	4.7	6.42	3.5	5.3	3.68	5.3	
H11	-6.2	-7.1	-7.9	-4.9	-5.3	-6.84	-7.2	-8.3	-7.0	-7.6	-8.2	-7.2	-10.1	-7.03	-8.9	
H12	-6.2	-7.0	-7.6	-4.8	-5.2	-6.84	-7.2	-8.2	-7.0	-7.6	-8.2	-7.2	-10.1	-7.03	-8.9	
H13	-6.2	-7.1	-8.1	-4.8	-5.3	-6.84	-7.3	-8.3	-7.1	-7.7	-8.2	-7.3	-10.2	-7.13	-9.0	
H14	-6.2	-7.0	-8.3	-4.7	-5.3	-6.84	-7.3	-8.2	-7.1	-7.7	-8.2	-7.3	-10.2	-7.13	-9.0	
H <sub>Cp</sub> *	1.81	1.9	1.9	1.4	1.4	1.93	1.7	1.9	1.7	1.7	2.08	1.6	2.0	1.45	1.9	
<i><sup>13</sup>C NMR</i>																
C <sub>Cp</sub>	108.1	106.6	106.5	109.4	109.3	na	108.8	107.9	-	111.8	na	107.4	107.5	110.7	110.5	
C <sub>Me</sub>	12.9	9.3	9.2	9.6	9.8	na	10.7	10.0	-	10.5	na	9.1	9.2	9.5	9.9	

**Table ST6**

DFT BP86/TZ2P and B3LYP/TZ2P computed (scalar/spin orbit ZORA) and experimental NMR chemical shifts  $\delta$  (ppm) for the compounds (Cp\* $M$ )<sub>2</sub>B<sub>3</sub>H<sub>7</sub> (**15** M = Co; **16** M = Rh; **16b** M = Rh).

Cmpd.	<b>15</b>				<b>16</b>				<b>16b</b>						
	Exp.	BP86/T Z2P/SC	BP86/T TZ2P/SC	B3LYP /TZ2P/ SO	Exp.	BP86/ TZ2P/ SC	BP86/T Z2P/SO	B3LYP /TZ2P/ SC	Exp.	BP86/T Z2P/SC	BP86/T Z2P/SO	B3LYP/ TZ2P/ SC	B3LYP/ TZ2P/ SO		
<b><sup>11</sup>B NMR</b>															
B3	-18.1	-17.1	21.0	-19.2	-25.6	na	5.3	1.0	9.6	5.3	na	-7.0	-13.4	-4.3	-12.9
B4	65.8	72.8	68.9	64.3	58.6	na	1.0	0.1	2.7	0.8	na	1.0	-0.4	3.2	1.5
B5	-18.1	-16.1	-20.6	-18.4	-24.8	na	6.4	3.9	10.4	5.0	na	52.2	47.3	56.8	48.5
<b><sup>1</sup>H NMR</b>															
H6	na	1.2	0.8	0.3	-0.2	3.7	3.0	2.8	2.8	2.7	2.7	2.3	1.9	2.1	1.7
H7	6.3	6.0	6.0	5.9	5.8	4.0	2.3	3.3	2.0	3.1	4.2	2.7	3.3	2.5	3.2
H8	na	1.3	0.9	0.4	-0.1	3.7	3.2	3.2	2.9	2.8	5.7	5.2	5.6	5.2	5.5
H9	-12.7	-7.6	-9.0	-11.9	-14.2	-12.0	-9.6	-11.6	-11.4	-14.3	-15.0	-11.8	-16.7	-13.9	-19.2
H10	-12.7	-7.6	-9.0	-11.6	-14.3	-3.1	-2.8	-3.6	-3.6	-4.6	-3.4	-3.1	-4.4	-4.0	-5.5
H11	-12.7	-7.6	-9.0	-11.5	-14.2	-3.1	-2.7	-3.9	-3.6	-5.0	-0.2	0.5	-0.7	-0.6	-1.9

H12	-12.7	-7.6	-9.0	-11.6	-14.3	-12.0	-9.5	-14.0	-11.3	-15.4	-14.5	-8.6	-9.8	-10.2	-14.6
H(Cp)	1.7	1.7	1.6	1.6	1.5	1.5	1.3	1.2	1.5	1.2	1.7	1.3	1.2	1.2	1.0
<i><sup>13</sup>C NMR</i>															
C <sub>Cp</sub>	10.3	5.6	5.5	5.4	5.5	na	6.9	6.5	6.7	6.6	na	7.1	7.0	6.6	6.7
C <sub>Me</sub>	89.6	94.4	94.6	93.5	94.2	na	90.3	89.9	91.5	91.0	na	86.7	85.5	86.1	84.7

**Cartesian coordinates for the optimized geometries of clusters 1-17.****1**

1.V	0.779443	0.561109	0.973806
2.V	-0.779443	-0.561109	-0.973806
3.B	-1.466686	0.771067	0.729884
4.B	-0.990940	-0.826116	1.270682
5.B	1.466686	-0.771067	-0.729884
6.B	0.990940	0.826116	-1.270682
7.H	-1.716783	0.883710	-0.516645
8.H	0.179198	-0.912912	1.773738
9.H	-2.453070	1.207383	1.273024
10.H	-1.712716	-1.301153	2.114297
11.H	-0.953772	-1.725220	0.358764
12.H	-0.591187	1.689946	0.907077
13.H	1.716783	-0.883710	0.516645
14.H	-0.179198	0.912912	-1.773738
15.H	2.453070	-1.207383	-1.273024
16.H	1.712716	1.301153	-2.114297
17.H	0.953772	1.725220	-0.358764
18.H	0.591187	-1.689946	-0.907077
19.C	1.055476	1.066402	3.173510
20.C	2.143318	0.251028	2.734162
21.C	2.883729	0.988652	1.760029
22.C	2.249294	2.242282	1.593323
23.C	1.121949	2.291160	2.462199
24.H	0.304603	0.793210	3.905580
25.H	2.384263	-0.741006	3.098845
26.H	3.761467	0.643003	1.226216
27.H	2.558705	3.025562	0.910263
28.H	0.431812	3.121857	2.558794
29.C	-1.055476	-1.066402	-3.173510
30.C	-2.143318	-0.251028	-2.734162
31.C	-2.883729	-0.988652	-1.760029

32.C -2.249294 -2.242282 -1.593323  
 33.C -1.121949 -2.291160 -2.462199  
 34.H -0.304603 -0.793210 -3.905580  
 35.H -2.384263 0.741006 -3.098845  
 36.H -3.761467 -0.643003 -1.226216  
 37.H -2.558705 -3.025562 -0.910263  
 38.H -0.431812 -3.121857 -2.558794

2

1.Nb 1.042179 1.022764 0.000000  
 2.Nb 2.299335 3.695379 0.000000  
 3.B 2.477897 1.978290 -1.674657  
 4.B 0.863466 2.739795 -1.674725  
 5.B 2.477897 1.978290 1.674657  
 6.B 0.863466 2.739795 1.674725  
 7.H 0.428194 2.942073 -2.783185  
 8.H 2.590280 0.826466 -1.095148  
 9.H 3.437756 2.637052 -1.101211  
 10.H -0.096467 2.081061 -1.101343  
 11.H 0.751225 3.891796 -1.095436  
 12.H 2.913433 1.775898 -2.782938  
 13.H 0.428194 2.942073 2.783185  
 14.H 2.590280 0.826466 1.095148  
 15.H 3.437756 2.637052 1.101211  
 16.H -0.096467 2.081061 1.101343  
 17.H 0.751225 3.891796 1.095436  
 18.H 2.913433 1.775898 2.782938  
 19.C 4.097129 5.207591 0.712993  
 20.C 2.862626 5.747432 1.158231  
 21.C 2.085088 6.071069 0.000000  
 22.C 4.097129 5.207591 -0.712993  
 23.C 2.862626 5.747432 -1.158231  
 24.H 4.903790 4.855489 1.347222  
 25.H 2.563194 5.887776 2.190609



26.H	1.106197	6.537511	0.000000
27.H	4.903790	4.855489	-1.347222
28.H	2.563194	5.887776	-2.190609
29.C	1.259973	-1.352597	0.000000
30.C	0.481950	-1.030191	-1.158224
31.C	-0.753388	-0.492242	-0.712991
32.C	0.481950	-1.030191	1.158224
33.C	-0.753388	-0.492242	0.712991
34.H	2.239604	-1.817466	0.000000
35.H	0.781663	-1.170032	-2.190571
36.H	-1.560616	-0.141412	-1.347204
37.H	0.781663	-1.170032	2.190571
38.H	-1.560616	-0.141412	1.347204

3

1.Ta	-0.650502	-0.508418	-1.218255
2.Ta	0.650502	0.508418	1.218255
3.B	0.766878	-1.688233	0.299174
4.B	-0.823492	-1.354144	1.007712
5.B	-0.766878	1.688233	-0.299174
6.B	0.823492	1.354144	-1.007712
7.H	-0.907005	-0.358473	1.842791
8.H	1.755291	-0.918675	0.663246
9.H	-1.298431	-2.264090	1.640338
10.H	0.870659	-1.609813	-0.996866
11.H	-1.791879	-1.056294	0.185253
12.H	1.202829	-2.788981	0.527305
13.H	0.907005	0.358473	-1.842791
14.H	-1.755291	0.918675	-0.663246
15.H	1.298431	2.264090	-1.640338
16.H	-0.870659	1.609813	0.996866
17.H	1.791879	1.056294	-0.185253
18.H	-1.202829	2.788981	-0.527305
19.C	-2.300656	-1.958057	-2.297426

20.C -1.027459 -2.323102 -2.797137  
 21.C -0.483587 -1.196722 -3.492579  
 22.C -1.441897 -0.133031 -3.431952  
 23.C -2.559912 -0.606202 -2.678732  
 24.C 1.027459 2.323102 2.797137  
 25.C 0.483587 1.196722 3.492579  
 26.C 1.441897 0.133031 3.431952  
 27.C 2.559912 0.606202 2.678732  
 28.C 2.300656 1.958057 2.297426  
 29.H -0.465429 1.172680 4.017233  
 30.H 1.345342 -0.844274 3.890395  
 31.H 3.464330 0.048475 2.460424  
 32.H 2.957534 2.590470 1.709490  
 33.H 0.542640 3.283899 2.661075  
 34.H 0.465429 -1.172680 -4.017233  
 35.H -1.345342 0.844274 -3.890395  
 36.H -3.464330 -0.048475 -2.460424  
 37.H -2.957534 -2.590470 -1.709490  
 38.H -0.542640 -3.283899 -2.661075

1'

1.V 0.778251 0.564673 0.972639  
 2.V -0.778251 -0.564673 -0.972639  
 3.B -1.470664 0.771053 0.731453  
 4.B -0.996181 -0.823945 1.273353  
 5.B 1.470664 -0.771053 -0.731453  
 6.B 0.996181 0.823945 -1.273353  
 7.H -1.721309 0.877116 -0.516359  
 8.H 0.174246 -0.904983 1.778186  
 9.H -2.460736 1.212414 1.269116  
 10.H -1.716222 -1.302788 2.119879  
 11.H -0.952312 -1.724318 0.364523  
 12.H -0.595334 1.689724 0.901249  
 13.H 1.721309 -0.877116 0.516359

14.H -0.174246 0.904983 -1.778186  
15.H 2.460736 -1.212414 -1.269116  
16.H 1.716222 1.302788 -2.119879  
17.H 0.952312 1.724318 -0.364523  
18.H 0.595334 -1.689724 -0.901249  
19.C -1.112395 -2.297537 -2.459536  
20.C -1.046490 -1.063290 -3.172456  
21.C -2.140605 -0.244008 -2.728576  
22.C -2.884594 -0.987996 -1.749904  
23.C -2.246171 -2.250055 -1.584468  
24.C 1.046490 1.063290 3.172456  
25.C 2.140605 0.244008 2.728576  
26.C 2.884594 0.987996 1.749904  
27.C 2.246171 2.250055 1.584468  
28.C 1.112395 2.297537 2.459536  
29.C 0.086831 0.732181 4.275336  
30.C 2.543916 -1.076997 3.315879  
31.C 4.169952 0.562993 1.106542  
32.C 2.749339 3.377186 0.732551  
33.C 0.231129 3.489866 2.688321  
34.C -0.086831 -0.732181 -4.275336  
35.C -2.543916 1.076997 -3.315879  
36.C -4.169952 -0.562993 -1.106542  
37.C -2.749339 -3.377186 -0.732551  
38.C -0.231129 -3.489866 -2.688321  
39.H -0.108058 -0.345420 4.332035  
40.H 0.491095 1.051509 5.249410  
41.H -0.878355 1.232460 4.133002  
42.H 3.060488 -1.706093 2.581070  
43.H 3.229157 -0.927462 4.165616  
44.H 1.676655 -1.637697 3.684295  
45.H 4.282409 0.996474 0.105628  
46.H 5.030618 0.887830 1.712936  
47.H 4.229394 -0.526767 1.000541  
48.H 1.941428 4.058793 0.440835  
49.H 3.498898 3.966167 1.284324  
50.H 3.223192 3.009216 -0.185541

51.H	-0.784929	3.192919	2.974284
52.H	0.638620	4.114413	3.498987
53.H	0.155898	4.118018	1.792523
54.H	0.108058	0.345420	-4.332035
55.H	0.878355	-1.232460	-4.133002
56.H	-0.491095	-1.051509	-5.249410
57.H	-3.060488	1.706093	-2.581070
58.H	-1.676655	1.637697	-3.684295
59.H	-3.229157	0.927462	-4.165616
60.H	-4.282409	-0.996474	-0.105628
61.H	-4.229394	0.526767	-1.000541
62.H	-5.030618	-0.887830	-1.712936
63.H	-1.941428	-4.058793	-0.440835
64.H	-3.223192	-3.009216	0.185541
65.H	-3.498898	-3.966167	-1.284324
66.H	0.784929	-3.192919	-2.974284
67.H	-0.155898	-4.118018	-1.792523
68.H	-0.638620	-4.114413	-3.498987

2'

1.Nb	1.036511	1.027264	-0.006728
2.Nb	2.306385	3.690153	-0.006908
3.B	2.477391	1.974765	-1.689647
4.B	0.865426	2.742497	-1.689663
5.B	2.477627	1.975175	1.674429
6.B	0.865343	2.742435	1.674443
7.H	0.432474	2.949290	-2.801197
8.H	2.579418	0.820896	-1.111218
9.H	3.439505	2.625956	-1.113578
10.H	-0.096639	2.091396	-1.113418
11.H	0.763440	3.896471	-1.111387
12.H	2.910270	1.767783	-2.801174
13.H	0.434640	2.951021	2.786684
14.H	2.582059	0.822657	1.093905

15.H 3.440355 2.627366 1.101137  
16.H -0.097420 2.090127 1.101347  
17.H 0.760850 3.894860 1.093751  
18.H 2.908461 1.766780 2.786647  
19.C -0.740391 -0.484154 0.747038  
20.C -0.773060 -0.472311 -0.689059  
21.C 0.461076 -1.009965 -1.169240  
22.C 1.270932 -1.342013 -0.023683  
23.C 0.513554 -1.027245 1.161662  
24.C 4.083430 5.201363 0.747019  
25.C 2.829481 5.744481 1.161647  
26.C 2.072272 6.059583 -0.023669  
27.C 2.882049 5.727425 -1.169248  
28.C 4.116145 5.189634 -0.689070  
29.C 5.221230 4.836715 1.657720  
30.C 2.430755 6.065672 2.573390  
31.C 0.773092 6.815537 -0.057221  
32.C 5.297903 4.815872 -1.538274  
33.C 2.550189 6.034751 -2.601155  
34.C 2.570205 -2.097823 -0.057234  
35.C 0.793000 -1.317070 -2.601175  
36.C -1.954805 -0.098567 -1.538295  
37.C 0.912224 -1.348637 2.573355  
38.C -1.878251 -0.119570 1.657691  
39.H 5.874681 4.079087 1.209587  
40.H 5.838987 5.722608 1.874071  
41.H 4.862181 4.440525 2.614763  
42.H 2.886172 5.372328 3.289965  
43.H 2.750185 7.084642 2.844702  
44.H 1.344555 6.011193 2.711149  
45.H 0.146713 6.584163 0.812311  
46.H 0.957462 7.902127 -0.053976  
47.H 0.190888 6.581559 -0.956106  
48.H 1.472112 5.972856 -2.790368  
49.H 2.876929 7.053276 -2.865592  
50.H 3.043224 5.337899 -3.288688  
51.H 4.987488 4.412926 -2.509368

52.H	5.927782	5.699064	-1.729447
53.H	5.925997	4.060772	-1.051268
54.H	3.196570	-1.866342	0.812282
55.H	2.386001	-3.184445	-0.053954
56.H	3.152375	-1.863796	-0.956132
57.H	1.871094	-1.255253	-2.790301
58.H	0.466165	-2.335509	-2.865804
59.H	0.300081	-0.620045	-3.288620
60.H	-1.644359	0.304478	-2.509346
61.H	-2.584626	-0.981786	-1.729570
62.H	-2.582972	0.656455	-1.051266
63.H	-2.531698	0.638037	1.209522
64.H	-2.495994	-1.005476	1.874020
65.H	-1.519256	0.276641	2.614748
66.H	0.456499	-0.655619	3.290036
67.H	0.593065	-2.367769	2.844361
68.H	1.998393	-1.293869	2.711258

3'

1.Ta	0.651235	0.505427	1.217561
2.Ta	-0.651235	-0.505427	-1.217561
3.B	-0.825323	-1.356629	1.005240
4.B	0.764463	-1.691157	0.296679
5.B	0.825323	1.356629	-1.005240
6.B	-0.764463	1.691157	-0.296679
7.H	0.867926	-1.609908	-0.999109
8.H	-1.793625	-1.054145	0.185708
9.H	1.198885	-2.795618	0.518658
10.H	-0.904659	-0.363339	1.843710
11.H	1.753448	-0.924214	0.662189
12.H	-1.303214	-2.268525	1.636301
13.H	-0.867926	1.609908	0.999109
14.H	1.793625	1.054145	-0.185708
15.H	-1.198885	2.795618	-0.518658

16.H 0.904659 0.363339 -1.843710  
17.H -1.753448 0.924214 -0.662189  
18.H 1.303214 2.268525 -1.636301  
19.C -0.780100 1.202406 4.321208  
20.H -1.210816 0.198577 4.413735  
21.H -1.549901 1.855909 3.893579  
22.H -0.562696 1.566301 5.338330  
23.C 1.361043 -1.171052 4.180520  
24.H 0.327369 -1.524270 4.272568  
25.H 1.767292 -1.057314 5.198613  
26.H 1.932803 -1.960877 3.679945  
27.C 3.862381 -0.127227 2.482593  
28.H 4.369661 0.176360 1.559139  
29.H 3.715286 -1.212667 2.439853  
30.H 4.544382 0.083657 3.321664  
31.C 3.246405 2.873544 1.560686  
32.H 3.947096 2.315351 0.928937  
33.H 3.840017 3.454992 2.283303  
34.H 2.714420 3.584507 0.917252  
35.C 0.393090 3.689210 2.689789  
36.H 0.662275 4.194577 1.754751  
37.H 0.731715 4.323623 3.523935  
38.H -0.701166 3.639888 2.734226  
39.C 1.014392 2.326025 2.781504  
40.C 0.470825 1.194762 3.487752  
41.C 1.437604 0.127223 3.430314  
42.C 2.561749 0.601447 2.670189  
43.C 2.296731 1.959704 2.279016  
44.C 0.780100 -1.202406 -4.321208  
45.H 1.210816 -0.198577 -4.413735  
46.H 1.549901 -1.855909 -3.893579  
47.H 0.562696 -1.566301 -5.338330  
48.C -1.361043 1.171052 -4.180520  
49.H -0.327369 1.524270 -4.272568  
50.H -1.767292 1.057314 -5.198613  
51.H -1.932803 1.960877 -3.679945  
52.C -3.862381 0.127227 -2.482593

53.H -4.369661 -0.176360 -1.559139  
54.H -3.715286 1.212667 -2.439853  
55.H -4.544382 -0.083657 -3.321664  
56.C -3.246405 -2.873544 -1.560686  
57.H -3.947096 -2.315351 -0.928937  
58.H -3.840017 -3.454992 -2.283303  
59.H -2.714420 -3.584507 -0.917252  
60.C -0.393090 -3.689210 -2.689789  
61.H -0.662275 -4.194577 -1.754751  
62.H -0.731715 -4.323623 -3.523935  
63.H 0.701166 -3.639888 -2.734226  
64.C -1.014392 -2.326025 -2.781504  
65.C -0.470825 -1.194762 -3.487752  
66.C -1.437604 -0.127223 -3.430314  
67.C -2.561749 -0.601447 -2.670189  
68.C -2.296731 -1.959704 -2.279016

4

1.Cr 0.788578 0.555247 0.986849  
2.Cr -0.788578 -0.555247 -0.986849  
3.B -1.486228 0.731848 0.775794  
4.B -1.037541 -0.797247 1.278335  
5.B 1.486228 -0.731848 -0.775794  
6.B 1.037541 0.797247 -1.278335  
7.H -1.659867 0.859864 -0.501501  
8.H 0.180721 -0.891164 1.710600  
9.H -2.451323 1.300123 1.233654  
10.H -1.662693 -1.405841 2.116752  
11.H -0.923260 -1.674972 0.332975  
12.H -0.562136 1.634075 0.886305  
13.H 1.659867 -0.859864 0.501501  
14.H -0.180721 0.891164 -1.710600  
15.H 2.451323 -1.300123 -1.233654  
16.H 1.662693 1.405841 -2.116752



17.H 0.923260 1.674972 -0.332975  
18.H 0.562136 -1.634075 -0.886305  
19.C -1.065616 -2.274551 -2.388229  
20.C -0.968027 -1.020447 -3.075041  
21.C -2.063459 -0.185616 -2.625598  
22.C -2.822246 -0.951630 -1.661044  
23.C -2.202871 -2.230020 -1.527809  
24.C 0.968027 1.020447 3.075041  
25.C 2.063459 0.185616 2.625598  
26.C 2.822246 0.951630 1.661044  
27.C 2.202871 2.230020 1.527809  
28.C 1.065616 2.274551 2.388229  
29.C -0.002760 0.699180 4.169907  
30.C 2.468452 -1.131662 3.215659  
31.C 4.104309 0.534570 1.007867  
32.C 2.707753 3.354564 0.676248  
33.C 0.180608 3.462822 2.613847  
34.C 0.002760 -0.699180 -4.169907  
35.C -2.468452 1.131662 -3.215659  
36.C -4.104309 -0.534570 -1.007867  
37.C -2.707753 -3.354564 -0.676248  
38.C -0.180608 -3.462822 -2.613847  
39.H -0.148130 -0.382242 4.272749  
40.H 0.361916 1.085385 5.135583  
41.H -0.986913 1.143559 3.977519  
42.H 2.992528 -1.755704 2.481325  
43.H 3.143626 -0.984944 4.074039  
44.H 1.597162 -1.696863 3.568482  
45.H 4.179595 0.921919 -0.015537  
46.H 4.966513 0.914599 1.579238  
47.H 4.191960 -0.556337 0.952680  
48.H 1.907188 4.053584 0.407515  
49.H 3.477655 3.921424 1.223044  
50.H 3.158093 2.984990 -0.252883  
51.H -0.846673 3.160238 2.849949  
52.H 0.559456 4.059486 3.458565  
53.H 0.144825 4.116610 1.734320

54.H 0.148130 0.382242 -4.272749  
 55.H 0.986913 -1.143559 -3.977519  
 56.H -0.361916 -1.085385 -5.135583  
 57.H -2.992528 1.755704 -2.481325  
 58.H -1.597162 1.696863 -3.568482  
 59.H -3.143626 0.984944 -4.074039  
 60.H -4.179595 -0.921919 0.015537  
 61.H -4.191960 0.556337 -0.952680  
 62.H -4.966513 -0.914599 -1.579238  
 63.H -1.907188 -4.053584 -0.407515  
 64.H -3.158093 -2.984990 0.252883  
 65.H -3.477655 -3.921424 -1.223044  
 66.H 0.846673 -3.160238 -2.849949  
 67.H -0.144825 -4.116610 -1.734320  
 68.H -0.559456 -4.059486 -3.458565

5

1.Mo 1.055657 1.045928 0.003736  
 2.Mo 2.285523 3.672209 0.003797  
 3.B 0.904816 2.717642 1.738378  
 4.B 2.435273 2.000285 1.738997  
 5.B 2.436102 1.999937 -1.730909  
 6.B 0.906006 2.717879 -1.731385  
 7.H 0.347271 2.984217 -2.772598  
 8.H 2.553988 0.868533 -1.065966  
 9.H 3.385778 2.643733 -1.085254  
 10.H -0.044031 2.074109 -1.085528  
 11.H 0.788141 3.849886 -1.067239  
 12.H 2.994366 1.732854 -2.772168  
 13.H 0.345126 2.984671 2.778749  
 14.H 2.552742 0.868334 1.075453  
 15.H 3.384820 2.644129 1.093130  
 16.H -0.044528 2.074140 1.091533  
 17.H 0.788729 3.850228 1.074636

18.H 2.993258 1.734275 2.780555  
19.C -0.724010 -0.348722 0.697491  
20.C -0.706961 -0.359772 -0.731272  
21.C 0.569639 -0.841889 -1.171373  
22.C 1.372344 -1.138630 0.012200  
23.C 0.542870 -0.826382 1.174755  
24.C 4.066341 5.064520 0.699154  
25.C 2.799299 5.542957 1.176049  
26.C 1.971307 5.857009 0.013253  
27.C 2.774434 5.559544 -1.170100  
28.C 4.050511 5.076630 -0.729392  
29.C 5.238234 4.699140 1.560808  
30.C 2.462641 5.836963 2.608139  
31.C 0.685565 6.630790 0.030921  
32.C 5.199243 4.720007 -1.625142  
33.C 2.402951 5.866514 -2.590761  
34.C 2.659118 -1.910734 0.031722  
35.C 0.943313 -1.146569 -2.592013  
36.C -1.855156 -0.003316 -1.627789  
37.C 0.880707 -1.122416 2.606132  
38.C -1.896311 0.016580 1.558853  
39.H -1.575449 0.463541 2.507044  
40.H -2.559256 0.732333 1.059329  
41.H -2.488423 -0.881866 1.793496  
42.H -2.531369 0.718290 -1.155422  
43.H -1.508213 0.431527 -2.572418  
44.H -2.440816 -0.904669 -1.867506  
45.H 0.506933 -0.420210 -3.287451  
46.H 2.029126 -1.121415 -2.735953  
47.H 0.587254 -2.148290 -2.881738  
48.H 3.275029 -1.681210 -0.846081  
49.H 3.254568 -1.670373 0.920566  
50.H 2.471677 -2.997064 0.035952  
51.H 1.380602 5.813165 2.778814  
52.H 2.913579 5.102633 3.285671  
53.H 2.828537 6.835050 2.898117  
54.H 4.917376 4.252335 2.509053

55.H 5.901692 3.983861 1.061345  
 56.H 5.829870 5.597920 1.795633  
 57.H 5.874587 3.997707 -1.152569  
 58.H 4.852971 4.286011 -2.570394  
 59.H 5.785639 5.621193 -1.863683  
 60.H 2.841002 5.141642 -3.286708  
 61.H 1.317448 5.841131 -2.736922  
 62.H 2.759141 6.868909 -2.877904  
 63.H 0.071821 6.403207 -0.848877  
 64.H 0.087253 6.389931 0.917753  
 65.H 0.874403 7.716874 0.037246  
 66.H 0.421702 -0.395179 3.285909  
 67.H 0.523704 -2.124967 2.891808  
 68.H 1.962210 -1.088837 2.778150

6

1.W 0.627657 0.486910 1.218354  
 2.W -0.627657 -0.486910 -1.218354  
 3.B -0.805137 -1.419474 0.993642  
 4.B 0.713784 -1.740852 0.335557  
 5.B 0.805137 1.419474 -0.993642  
 6.B -0.713784 1.740852 -0.335557  
 7.H 0.850816 -1.573170 -0.968868  
 8.H -1.748462 -1.030234 0.155955  
 9.H 1.238563 -2.814760 0.487050  
 10.H -0.897702 -0.379205 1.801355  
 11.H 1.692725 -0.930088 0.683173  
 12.H -1.394838 -2.258366 1.626306  
 13.H -0.850816 1.573170 0.968868  
 14.H 1.748462 1.030234 -0.155955  
 15.H -1.238563 2.814760 -0.487050  
 16.H 0.897702 0.379205 -1.801355  
 17.H -1.692725 0.930088 -0.683173  
 18.H 1.394838 2.258366 -1.626306

19.C 1.187260 4.222268  
20.H 0.198440 4.290816  
21.H 1.887741 3.847644  
22.H 1.500532 5.244318  
23.C -1.214571 4.047349  
24.H -1.567461 4.177229  
25.H -1.078476 5.049673  
26.H -2.015216 3.544067  
27.C -0.151518 2.345829  
28.H 0.195980 1.457085  
29.H -1.233595 2.244090  
30.H 0.016611 3.219853  
31.C 2.857764 1.473666  
32.H 2.301843 0.833095  
33.H 3.422010 2.205860  
34.H 3.582002 0.844516  
35.C 3.672654 2.588614  
36.H 4.184450 1.659636  
37.H 4.294017 3.431318  
38.H 3.628211 2.628454  
39.C 2.306021 2.674888  
40.C 1.157311 3.337479  
41.C 0.063305 3.261057  
42.C 0.565943 2.518165  
43.C 1.943117 2.187767  
44.C -1.187260 -4.222268  
45.H -0.198440 -4.290816  
46.H -1.887741 -3.847644  
47.H -1.500532 -5.244318  
48.C 1.214571 -4.047349  
49.H 1.567461 -4.177229  
50.H 1.078476 -5.049673  
51.H 2.015216 -3.544067  
52.C 0.151518 -2.345829  
53.H -0.195980 -1.457085  
54.H 1.233595 -2.244090  
55.H -0.016611 -3.219853

56.C -3.207176 -2.857764 -1.473666  
57.H -3.901174 -2.301843 -0.833095  
58.H -3.805269 -3.422010 -2.205860  
59.H -2.676348 -3.582002 -0.844516  
60.C -0.363118 -3.672654 -2.588614  
61.H -0.641504 -4.184450 -1.659636  
62.H -0.704597 -4.294017 -3.431318  
63.H 0.731091 -3.628211 -2.628454  
64.C -0.974387 -2.306021 -2.674888  
65.C -0.384962 -1.157311 -3.337479  
66.C -1.359638 -0.063305 -3.261057  
67.C -2.509447 -0.565943 -2.518165  
68.C -2.257908 -1.943117 -2.187767

7

1.B 12.178911 6.263173 2.867862  
2.B 11.158875 4.948524 3.302518  
3.B 11.148522 4.279777 4.844639  
4.B 12.155386 4.885691 6.046196  
5.B 13.234317 6.197521 5.778931  
6.H 12.097567 6.657890 1.730474  
7.H 10.418972 4.494864 2.466720  
8.H 10.415430 3.360131 5.089982  
9.H 12.127022 4.378119 7.138463  
10.H 13.908129 6.544473 6.717934  
11.H 13.437289 5.993603 3.032775  
12.H 11.969369 7.316496 3.597196  
13.H 12.622505 7.276625 5.398074  
14.H 14.089522 5.952240 4.833728  
15.Cr 13.093951 4.722350 4.147991  
16.Cr 11.242795 6.391877 4.857988  
17.C 14.754088 3.415676 4.776306  
18.C 13.592022 2.597610 4.622258  
19.C 13.169274 2.678334 3.251158

20.C 14.071884 3.544873 2.561654  
21.C 15.053376 4.003979 3.502396  
22.C 15.574360 3.546773 6.023332  
23.H 14.948252 3.487794 6.921341  
24.H 16.112958 4.501214 6.056684  
25.H 16.321841 2.739462 6.076899  
26.C 13.034681 1.666992 5.654550  
27.H 11.960998 1.501367 5.509804  
28.H 13.179385 2.056249 6.668976  
29.H 13.541563 0.690306 5.588898  
30.C 12.091214 1.851917 2.620964  
31.H 11.688273 2.331783 1.721710  
32.H 11.256884 1.684564 3.312141  
33.H 12.494973 0.868504 2.329425  
34.C 14.050494 3.839872 1.092729  
35.H 13.024460 3.889090 0.709305  
36.H 14.582789 3.052485 0.536285  
37.H 14.536498 4.795437 0.863199  
38.C 16.251790 4.847809 3.181378  
39.H 16.047630 5.548899 2.363743  
40.H 17.095317 4.211536 2.870666  
41.H 16.580021 5.432468 4.048499  
42.C 10.298702 7.636690 6.413587  
43.C 10.217965 8.300375 5.143750  
44.C 9.422943 7.486952 4.269471  
45.C 9.015190 6.325832 4.997392  
46.C 9.558570 6.418142 6.324532  
47.C 10.959601 8.169010 7.648618  
48.H 11.768326 8.868666 7.407035  
49.H 11.389252 7.361076 8.252760  
50.H 10.228493 8.706431 8.272704  
51.C 10.762361 9.662316 4.827358  
52.H 11.682372 9.871937 5.385383  
53.H 10.028105 10.438793 5.093559  
54.H 10.986998 9.770978 3.760024  
55.C 8.999241 7.841489 2.876694  
56.H 8.873334 6.945600 2.257500

57.H	9.733672	8.486986	2.380638
58.H	8.038554	8.380232	2.893969
59.C	8.031982	5.299853	4.524953
60.H	8.190194	4.333514	5.016980
61.H	8.103977	5.140142	3.442836
62.H	7.006478	5.633690	4.752877
63.C	9.246200	5.494535	7.461142
64.H	9.141381	4.457916	7.120013
65.H	8.298758	5.794028	7.938381
66.H	10.031048	5.515589	8.225898

8

1.B	0.388513	-1.830125	0.022532
2.B	-1.285740	-1.237462	0.018933
3.B	-1.714868	0.444768	0.003133
4.B	-0.518853	1.701127	-0.020934
5.B	1.230324	1.399741	-0.023912
6.H	0.553141	-3.026487	0.033870
7.H	-2.171719	-2.060900	0.036614
8.H	-2.882693	0.748771	0.011639
9.H	-0.887006	2.853353	-0.034848
10.H	1.957927	2.363428	-0.037332
11.H	1.096806	-1.431260	-1.018419
12.H	1.100204	-1.408752	1.052742
13.H	1.642321	0.683008	-1.055307
14.H	1.656443	0.707114	1.016187
15.Mo	-0.055897	-0.011446	-1.409676
16.Mo	-0.042663	0.027351	1.407422
17.C	-1.284293	-0.865635	-3.274660
18.C	0.113866	-0.968155	-3.576469
19.C	0.658833	0.363719	-3.634118
20.C	-0.405105	1.292466	-3.367817
21.C	-1.599185	0.529243	-3.130368
22.C	-2.276767	-1.991340	-3.268351



23.H -3.082020 -1.810321 -2.547901  
24.H -1.805873 -2.942070 -2.993578  
25.H -2.729639 -2.115896 -4.265794  
26.C 0.863638 -2.239591 -3.861774  
27.H 0.782080 -2.514097 -4.925513  
28.H 0.476378 -3.076013 -3.268607  
29.H 1.929899 -2.139913 -3.627389  
30.C 2.073727 0.723563 -3.997406  
31.H 2.781992 -0.051781 -3.683093  
32.H 2.384365 1.660584 -3.521660  
33.H 2.180824 0.849300 -5.086595  
34.C -0.323033 2.788796 -3.467252  
35.H -1.015721 3.273740 -2.770102  
36.H -0.569078 3.127305 -4.487286  
37.H 0.683035 3.154392 -3.229979  
38.C -2.977710 1.093258 -2.971860  
39.H -3.455911 1.229961 -3.954780  
40.H -2.954780 2.063375 -2.465826  
41.H -3.611527 0.432146 -2.372946  
42.C -1.670473 0.064307 3.145074  
43.C -0.928134 1.291469 3.239519  
44.C 0.433641 0.959789 3.538201  
45.C 0.532780 -0.473861 3.638635  
46.C -0.774460 -1.027299 3.402851  
47.C -3.158076 -0.039128 2.998967  
48.H -3.650068 0.028242 3.982348  
49.H -3.446974 -0.988856 2.537390  
50.H -3.551414 0.761175 2.364541  
51.C -1.515229 2.671200 3.188251  
52.H -2.349218 2.723150 2.479810  
53.H -0.773985 3.412088 2.868788  
54.H -1.889015 2.971821 4.180800  
55.C 1.547833 1.939890 3.776355  
56.H 1.557285 2.278060 4.824728  
57.H 1.446568 2.824708 3.136949  
58.H 2.526959 1.495001 3.563626  
59.C 1.765635 -1.249646 4.015355

60.H	1.849426	-1.350064	5.109295
61.H	2.678036	-0.758842	3.657363
62.H	1.750452	-2.258950	3.589162
63.C	-1.156787	-2.474085	3.531512
64.H	-0.323192	-3.136160	3.268669
65.H	-1.992034	-2.726484	2.868565
66.H	-1.456119	-2.710501	4.565735

9

1.B	-0.905984	-1.602392	0.000000
2.B	0.838132	-1.515062	0.000000
3.B	1.694402	-0.022144	0.000000
4.B	0.875059	1.491720	0.000000
5.B	-0.866359	1.623163	0.000000
6.H	-1.408408	-2.696458	0.000000
7.H	1.473158	-2.537681	0.000000
8.H	2.895074	-0.034862	0.000000
9.H	1.534421	2.498688	0.000000
10.H	-1.338778	2.730599	0.000000
11.H	-1.498645	-1.013837	-1.048729
12.H	-1.498645	-1.013837	1.048729
13.H	-1.473885	1.049919	-1.048125
14.H	-1.473885	1.049919	1.048125
15.W	-0.004879	0.000052	-1.417621
16.W	-0.004879	0.000052	1.417621
17.C	-0.663961	0.000567	-3.660470
18.C	0.160607	-1.162478	-3.453749
19.C	1.484034	-0.714881	-3.127239
20.C	1.481236	0.724972	-3.127182
21.C	0.156125	1.166615	-3.453159
22.C	-2.078823	-0.001273	-4.167662
23.H	-2.088983	0.000551	-5.269078
24.H	-2.633288	0.882688	-3.831093
25.H	-2.630154	-0.888136	-3.833784

26.C	-0.251449	-2.588804	-3.673310
27.H	0.290978	-3.268046	-3.005509
28.H	-0.042000	-2.894372	-4.710539
29.H	-1.323383	-2.733950	-3.494654
30.C	2.694112	-1.587297	-2.981413
31.H	3.427465	-1.142999	-2.298536
32.H	3.179887	-1.727432	-3.960640
33.H	2.431599	-2.575584	-2.587033
34.C	2.687353	1.602418	-2.977876
35.H	3.418388	1.163157	-2.289259
36.H	2.419184	2.591074	-2.588247
37.H	3.178285	1.741425	-3.954682
38.C	-0.262313	2.591917	-3.667865
39.H	0.274513	3.271103	-2.995383
40.H	-1.335541	2.731218	-3.492410
41.H	-0.050621	2.903136	-4.702897
42.C	-0.663961	0.000567	3.660470
43.C	0.156125	1.166615	3.453159
44.C	1.481236	0.724972	3.127182
45.C	1.484034	-0.714881	3.127239
46.C	0.160607	-1.162478	3.453749
47.C	-2.078823	-0.001273	4.167662
48.H	-2.088983	0.000551	5.269078
49.H	-2.630154	-0.888136	3.833784
50.H	-2.633288	0.882688	3.831093
51.C	-0.262313	2.591917	3.667865
52.H	0.274513	3.271103	2.995383
53.H	-0.050621	2.903136	4.702897
54.H	-1.335541	2.731218	3.492410
55.C	2.687353	1.602418	2.977876
56.H	3.418388	1.163157	2.289259
57.H	3.178285	1.741425	3.954682
58.H	2.419184	2.591074	2.588247
59.C	2.694112	-1.587297	2.981413
60.H	3.427465	-1.142999	2.298536
61.H	2.431599	-2.575584	2.587033
62.H	3.179887	-1.727432	3.960640

63.C	-0.251449	-2.588804	3.673310
64.H	0.290978	-3.268046	3.005509
65.H	-1.323383	-2.733950	3.494654
66.H	-0.042000	-2.894372	4.710539

## 10

Cr	-4.414531	6.648116	12.765906
Cr	-6.092263	4.730283	12.760217
B	-5.222909	5.656698	14.531531
B	-4.103143	4.682579	13.632537
B	-4.060330	4.649658	11.996977
B	-5.128664	5.587817	11.002218
H	-5.232463	5.661415	15.738868
H	-3.367198	4.015093	14.315569
H	-3.293969	3.955481	11.376771
H	-5.059480	5.563376	9.796921
H	-6.376713	5.328012	11.209405
H	-5.106736	6.859076	11.252321
H	-5.144156	6.918433	14.257483
H	-6.462383	5.425833	14.247386
C	-2.357108	7.204562	13.386037
C	-3.283811	8.143955	13.939178
C	-3.979921	8.791006	12.855746
C	-3.427622	8.282323	11.633685
C	-2.446890	7.287725	11.956112
C	-6.891040	3.021330	13.933273
C	-7.991670	3.836143	13.481016
C	-7.990790	3.826718	12.058197
C	-6.890870	3.000736	11.620835
C	-6.215381	2.507276	12.781277
C	-9.021773	4.489878	14.355632
C	-9.021657	4.465077	11.173683
C	-6.574297	2.624926	10.206016
C	-5.109292	1.496403	12.792301

C -6.574499 2.671466 15.354953  
 C -3.416829 8.480680 15.394518  
 C -4.964377 9.917249 12.984204  
 C -3.742412 8.785729 10.255711  
 C -1.556478 6.576055 10.983666  
 C -1.347589 6.403310 14.150682  
 H -9.865477 3.804214 14.534184  
 H -9.426597 5.399356 13.894601  
 H -8.609277 4.766499 15.333519  
 H -9.862813 3.774319 11.002008  
 H -8.608815 4.731489 10.193104  
 H -9.430600 5.378682 11.622679  
 H -5.491108 2.543043 10.049678  
 H -6.955943 3.365571 9.493041  
 H -7.027686 1.652616 9.954374  
 H -5.528319 0.476815 12.810446  
 H -4.466487 1.615551 13.672266  
 H -4.474070 1.587069 11.903606  
 H -6.955300 3.425763 16.053846  
 H -5.491312 2.592349 15.512689  
 H -7.028466 1.704306 15.625109  
 H -3.281637 7.595646 16.028197  
 H -4.400218 8.908571 15.625811  
 H -2.654683 9.221672 15.683481  
 H -4.449384 10.891746 13.024060  
 H -5.566209 9.826424 13.896858  
 H -5.658218 9.945866 12.135144  
 H -4.762870 9.183626 10.190736  
 H -3.641902 7.995680 9.501942  
 H -3.050990 9.599039 9.984574  
 H -0.614561 7.132320 10.847431  
 H -2.031260 6.473420 10.000714  
 H -1.307465 5.567701 11.335666  
 H -1.694602 6.178686 15.166021  
 H -0.400449 6.961798 14.232710  
 H -1.137409 5.448090 13.655288

11

1.Cr	-6.328604	4.797600	12.669710
2.Cr	-4.526694	6.890786	12.786073
3.B	-5.756602	6.015942	14.371263
4.B	-4.523174	4.981982	13.820237
5.B	-4.208351	4.848276	12.204256
6.B	-5.142109	5.711009	11.073151
7.H	-6.182448	6.076604	15.493923
8.H	-3.929137	4.414937	14.700487
9.H	-3.362171	4.150465	11.708160
10.H	-4.908472	5.817876	9.898674
11.H	-6.424725	5.396593	11.097708
12.H	-5.565554	7.283501	14.052776
13.C	-6.072121	2.573925	12.459749
14.C	-6.554919	2.864073	13.781191
15.C	-7.827979	3.501916	13.657400
16.C	-8.134620	3.621437	12.251745
17.C	-7.046279	3.044687	11.520543
18.C	-3.692179	8.917483	12.907732
19.C	-3.273035	8.188511	14.067244
20.C	-2.458718	7.090207	13.638682
21.C	-2.376422	7.133244	12.205142
22.C	-3.129084	8.260732	11.751958
23.C	-1.664937	6.186207	14.530509
24.C	-3.545440	8.562644	15.493893
25.C	-4.435265	10.220236	12.909767
26.C	-3.174865	8.762626	10.339793
27.C	-1.479843	6.289007	11.351601
28.C	-5.946147	2.383102	15.063056
29.C	-8.751423	3.823485	14.794188
30.C	-9.429183	4.102705	11.666962
31.C	-6.975844	2.863243	10.033352
32.C	-4.871344	1.740253	12.134161
33.H	-9.331009	2.928584	15.071421

34.H -9.464113 4.614424 14.534024  
 35.C -7.493266 6.143654 13.147593  
 36.C -5.773798 7.648129 11.659714  
 37.H -8.196659 4.150386 15.682082  
 38.H -10.145202 3.269554 11.587271  
 39.H -9.287719 4.516581 10.661438  
 40.H -9.891243 4.882619 12.283006  
 41.H -5.949495 2.975430 9.663046  
 42.H -7.602110 3.592009 9.505717  
 43.H -7.327054 1.857167 9.755186  
 44.H -5.135399 0.671056 12.186267  
 45.H -4.050639 1.923098 12.837199  
 46.H -4.496346 1.945619 11.125248  
 47.H -6.135579 3.079458 15.888614  
 48.H -4.861524 2.258847 14.973754  
 49.H -6.379429 1.407103 15.337596  
 50.H -3.672014 7.674439 16.124868  
 51.H -4.453282 9.169940 15.587213  
 52.H -2.707156 9.149460 15.901014  
 53.H -3.728840 11.062180 12.981179  
 54.H -5.123335 10.290195 13.760657  
 55.H -5.025447 10.355637 11.996241  
 56.H -4.068216 9.367758 10.147163  
 57.H -3.168665 7.935328 9.619677  
 58.H -2.293951 9.391817 10.135690  
 59.H -0.507139 6.792039 11.223067  
 60.H -1.906803 6.122667 10.355455  
 61.H -1.296785 5.308255 11.803705  
 62.H -2.137648 6.067260 15.511914  
 63.H -0.658562 6.608046 14.687947  
 64.H -1.551046 5.187515 14.093631  
 65.O -6.486287 8.272828 10.962801  
 66.O -8.355888 6.894873 13.420908

1.Cr 12.738848  
2.Cr 12.749237  
3.B 11.031228  
4.B 12.013302  
5.B 13.649218  
6.B 14.456068  
7.H 15.661000  
8.H 14.382637  
9.H 11.402650  
10.H 9.825287  
11.H 11.269097  
12.H 11.299155  
13.H 14.117431  
14.H 14.090788  
15.H 14.710569  
16.H 14.084935  
17.C 13.463483  
18.C 13.938091  
19.C 12.802696  
20.C 11.623681  
21.C 12.027924  
22.C 13.904957  
23.C 13.546444  
24.C 12.117025  
25.C 11.592923  
26.C 12.695955  
27.C 14.498120  
28.C 11.313902  
29.C 10.149027  
30.C 12.611060  
31.C 15.294113  
32.C 15.375637  
33.C 12.844385  
34.C 10.213388  
35.C 11.122424  
36.C 14.308709  
37.H 12.631897

4.774628  
6.826442  
5.727159  
4.806091  
4.867226  
5.850681  
5.899522  
4.214089  
4.108422  
5.698665  
5.504452  
7.034499  
7.137140  
5.638286  
3.250946  
4.905161  
7.093601  
8.179025  
8.887249  
8.241322  
7.131759  
2.929109  
3.582328  
3.603705  
2.957955  
2.539776  
4.058790  
4.091996  
2.665061  
1.670830  
2.576719  
8.569309  
10.174868  
8.713515  
6.295996  
6.212194  
5.910586

-6.289813  
-4.480578  
-5.290013  
-4.250953  
-4.329349  
-5.459566  
-5.524952  
-3.628132  
-3.479278  
-5.231047  
-6.580235  
-5.263931  
-5.374299  
-6.724650  
-9.728093  
-9.571523  
-2.392100  
-3.196327  
-3.711132  
-3.212423  
-2.402140  
-6.728849  
-7.953581  
-8.043269  
-6.875081  
-6.065180  
-9.010217  
-9.211780  
-6.599660  
-4.848140  
-6.290746  
-3.370198  
-4.480432  
-3.406980  
-1.550115  
-1.524652  
-7.390486



38.H -5.740176 7.775144 12.661255  
 39.H -8.578321 4.379048 15.453649  
 40.H -9.925626 3.272179 11.136278  
 41.H -8.897729 4.476124 10.336140  
 42.H -9.746132 4.897422 11.830651  
 43.H -5.526615 2.718333 9.928421  
 44.H -7.110942 3.373596 9.486613  
 45.H -6.950191 1.652897 9.891216  
 46.H -5.145358 0.610194 12.663541  
 47.H -4.152403 1.872301 13.433665  
 48.H -4.306415 1.825753 11.671364  
 49.H -6.698123 3.273318 16.036423  
 50.H -5.198194 2.595472 15.384667  
 51.H -6.638446 1.564508 15.557162  
 52.H -3.427033 7.688573 16.026800  
 53.H -4.282996 9.157324 15.528937  
 54.H -2.518049 9.181563 15.710613  
 55.H -3.790459 11.032630 12.882739  
 56.H -5.129848 10.228717 13.725764  
 57.H -5.114918 10.294343 11.958800  
 58.H -4.341390 9.276076 10.099556  
 59.H -3.433324 7.874153 9.508143  
 60.H -2.579633 9.376787 9.915292  
 61.H -0.570899 6.781208 10.975429  
 62.H -2.012976 6.164603 10.137279  
 63.H -1.376404 5.298481 11.541065  
 64.H -1.957767 6.050033 15.302469  
 65.H -0.534181 6.678491 14.441449  
 66.H -1.379729 5.228887 13.847284

13

1.B -0.302045 7.215541 10.505028  
 2.B -1.668027 6.204304 10.352312  
 3.B 1.369755 6.786852 10.511129

4.B	0.607724	7.599980	11.920753
5.H	0.071912	4.694605	12.172734
6.H	-0.753828	8.066766	9.776903
7.H	1.588372	5.541316	10.792599
8.H	2.159421	7.214838	9.713124
9.H	1.867569	7.227166	11.667299
10.H	0.756890	8.723202	12.317894
11.H	0.457101	6.748705	12.889489
12.H	-2.680053	6.370236	9.731984
13.Cr	-0.971701	6.043682	12.241424
14.Cr	-0.032743	5.033149	10.501817
15.C	-2.910350	7.024323	12.926170
16.C	-1.881632	7.325474	13.861788
17.C	-1.391513	6.081770	14.411387
18.C	-2.149974	5.022341	13.820149
19.C	-3.072883	5.596246	12.891477
20.C	0.910326	3.110411	9.971854
21.C	-0.523767	2.992648	9.963282
22.C	-1.033577	3.843085	8.924280
23.C	0.090222	4.457882	8.270632
24.C	1.274974	3.990452	8.898085
25.C	0.015024	5.365319	7.080019
26.C	-2.443966	3.852059	8.414705
27.C	-1.318606	2.007686	10.768400
28.C	1.855879	2.307981	10.818709
29.C	2.674673	4.326654	8.481599
30.C	-1.464887	8.696723	14.299537
31.C	-0.409954	5.936836	15.537804
32.C	-2.058638	3.574392	14.202436
33.C	-4.154758	4.865115	12.153925
34.C	-3.769161	8.019257	12.206334
35.H	-0.895148	5.977052	7.100754
36.H	0.005700	4.782098	6.144938
37.H	0.872033	6.048235	7.037517
38.H	-2.580361	3.049262	7.671626
39.H	-2.696100	4.802922	7.931912
40.H	-3.170042	3.688377	9.219782

41.H	-1.344300	1.028998	10.261279
42.H	-2.356280	2.335702	10.899750
43.H	-0.885770	1.850481	11.763419
44.H	2.792724	2.847502	11.005059
45.H	2.115195	1.355038	10.329162
46.H	1.416171	2.068105	11.794328
47.H	2.999968	3.654211	7.672306
48.H	3.384454	4.214525	9.309960
49.H	2.753246	5.355879	8.111986
50.H	-0.415899	8.722821	14.617080
51.H	-2.079910	9.030908	15.150274
52.H	-1.580298	9.430943	13.493796
53.H	-0.923528	5.957319	16.512886
54.H	0.329086	6.747333	15.538391
55.H	0.139442	4.989260	15.475188
56.H	-2.403702	2.917074	13.396965
57.H	-2.685727	3.373783	15.086001
58.H	-1.031541	3.284098	14.455596
59.H	-5.091291	4.881776	12.734742
60.H	-3.892248	3.813584	11.986530
61.H	-4.360019	5.321178	11.178123
62.H	-4.640791	8.292103	12.823284
63.H	-4.143166	7.616129	11.257816
64.H	-3.217914	8.940136	11.981113
1.Cr	0.574707	0.888768	0.733932
2.Cr	-0.800903	-0.113375	-0.984676
3.B	-1.614670	1.273460	0.550208
4.B	-1.071133	-0.276190	1.021473
5.B	1.227332	-0.201170	-0.856168
6.B	0.811143	1.351417	-1.434110
7.H	-1.864816	1.371377	-0.694134
8.H	-2.597378	1.539440	1.196886

9.H 1.834891  
10.H 0.725335  
11.H -1.922136  
12.H -1.145643  
13.H -2.261374  
14.H -0.497105  
15.C -1.897092  
16.C -2.949880  
17.C -2.718283  
18.C -1.519246  
19.C -1.008027  
20.C 2.941311  
21.C 2.276676  
22.C 1.467962  
23.C 1.614409  
24.C 2.526009  
25.C 4.020605  
26.C 2.481004  
27.C 0.813025  
28.C 1.019978  
29.C 3.046558  
30.C -4.133564  
31.C -3.601231  
32.C -0.947066  
33.C 0.055843  
34.C -1.884033  
35.H 3.939996  
36.H 5.009487  
37.H 3.985685  
38.H 1.591716  
39.H 3.324224  
40.H 2.705339  
41.H -0.109708  
42.H 1.499134  
43.H 0.555487  
44.H 0.936376  
45.H 1.646118

-1.056336  
2.173729  
1.418139  
-0.944530  
1.679876  
2.221664  
-2.092239  
-1.151260  
-0.588358  
-1.154987  
-2.096553  
0.687641  
-0.233193  
0.512272  
1.901552  
2.006793  
0.355106  
-1.718316  
-0.023527  
3.038599  
3.279465  
-0.891116  
0.407920  
-0.902104  
-3.122119  
-3.104767  
-0.677706  
0.474628  
1.011398  
-2.238328  
-1.977079  
-2.109871  
0.518010  
0.076276  
-1.083233  
3.946520  
3.280868

-1.482629  
-0.722466  
-0.362646  
2.122430  
1.624990  
0.771206  
-0.586796  
-0.855536  
-2.148078  
-2.681489  
-1.721070  
0.827858  
1.704050  
2.627462  
2.301035  
1.193132  
-0.157328  
1.729307  
3.864881  
3.078099  
0.591998  
0.025143  
-2.842213  
-4.042809  
-1.978309  
0.519618  
-0.512925  
0.314436  
-1.035303  
2.105132  
2.389960  
0.730162  
4.105538  
4.721841  
3.762183  
2.468803  
3.951598

46.H	3.445015	2.791391	0.016258
47.H	-0.474058	3.158473	3.272986
48.H	1.097051	3.592170	3.974287
49.H	0.688714	4.099836	2.325403
50.H	-0.097330	0.130511	-4.513469
51.H	1.083126	-1.023114	-3.878456
52.H	-0.215925	-1.583945	-4.955717
53.H	-3.521977	1.052642	-3.031987
54.H	-2.128697	1.051634	-4.128719
55.H	-3.442417	-0.114693	-4.362854
56.H	-4.044394	-1.022539	0.142732
57.H	-4.392725	0.114011	-1.166469
58.H	-4.778380	-1.606138	-1.368073
59.H	-1.060660	-3.391625	0.592218
60.H	-2.703153	-2.769287	0.797437
61.H	-2.381315	-4.040215	-0.402850
62.H	1.407916	-2.747144	-2.415445
63.H	0.824657	-3.360344	-0.862170
64.H	0.180925	-4.032215	-2.374609
1.B	0.094200	-1.292325	-0.011716
2.B	-1.156421	-0.062656	-0.013095
3.B	-0.102996	1.337113	-0.018302
4.H	-0.119800	-2.482859	-0.009343
5.H	-2.360038	-0.148832	-0.012478
6.H	-0.484803	2.484728	-0.021038
7.H	0.995168	-1.010066	-0.932215
8.H	0.831841	1.185302	-0.938071
9.H	0.996606	-1.006774	0.906019
10.H	0.833558	1.189478	0.900153
11.CO	-0.037645	0.016795	-1.695728
12.CO	-0.034155	0.025557	1.666625
13.C	-0.037237	-1.166572	-3.378055

14.C 0.735847 0.019934 -3.630139  
15.C -0.120606 1.152782 -3.409427  
16.C -1.427593 0.670506 -3.032010  
17.C -1.375920 -0.770929 -3.014957  
18.C -0.057426 1.155709 3.386790  
19.C 0.748884 -0.014514 3.596095  
20.C -0.077462 -1.165018 3.341849  
21.C -1.399480 -0.708767 2.990497  
22.C -1.386569 0.733433 3.012754  
23.C 2.181145 -0.033976 4.039409  
24.C 0.341458 -2.598556 3.454021  
25.C -2.593616 -1.577728 2.745564  
26.C -2.563443 1.630040 2.784290  
27.C 0.382421 2.577716 3.555018  
28.C 2.164732 0.065747 -4.082399  
29.C 0.255292 2.593645 -3.571137  
30.C -2.642327 1.513259 -2.796807  
31.C -2.527374 -1.693524 -2.762103  
32.C 0.443171 -2.579929 -3.500076  
33.H 2.251623 -0.051064 5.139039  
34.H 2.724216 0.851577 3.687771  
35.H 2.708747 -0.917840 3.661228  
36.H -0.123247 -3.211993 2.672066  
37.H 0.043553 -3.013774 4.429925  
38.H 1.428570 -2.709701 3.362808  
39.H -3.281965 -1.115994 2.028015  
40.H -3.144103 -1.748850 3.685077  
41.H -2.302174 -2.555734 2.344356  
42.H -2.253263 2.606261 2.392747  
43.H -3.108035 1.802158 3.727052  
44.H -3.263525 1.190458 2.063948  
45.H -0.084192 3.230818 2.807001  
46.H 1.469860 2.678911 3.455798  
47.H 0.101221 2.954499 4.551327  
48.H 2.228908 0.052457 -5.182493  
49.H 2.734342 -0.793515 -3.708361  
50.H 2.669433 0.974810 -3.733552

51.H -0.229382 3.219834 -2.811612  
 52.H -0.054327 2.965916 -4.560655  
 53.H 1.338481 2.740893 -3.484150  
 54.H -2.373952 2.503608 -2.409913  
 55.H -3.316845 1.044342 -2.070657  
 56.H -3.200289 1.657884 -3.736365  
 57.H -3.233850 -1.260693 -2.044131  
 58.H -2.188932 -2.654788 -2.357240  
 59.H -3.072793 -1.894994 -3.698525  
 60.H 0.011886 -3.216390 -2.717275  
 61.H 1.534850 -2.643799 -3.418457  
 62.H 0.155399 -3.003865 -4.475279

## 16

1.Rh 5.209461 1.388461 5.406134  
 2.Rh 6.427074 2.934151 3.499208  
 3.B 4.777555 3.557494 4.636059  
 4.B 6.384042 4.321636 5.050832  
 5.B 7.134748 2.704524 5.457996  
 6.H 3.794086 4.108086 4.195191  
 7.H 6.830096 5.429754 4.914556  
 8.H 8.285146 2.485039 5.762847  
 9.H 4.327158 2.807497 5.665267  
 10.H 5.182606 4.470782 5.576817  
 11.H 6.899393 3.857455 6.170081  
 12.H 6.396246 2.071183 6.398319  
 13.C 3.973516 -0.240946 4.516024  
 14.C 3.417625 0.139771 5.798838  
 15.C 4.380534 -0.141326 6.822504  
 16.C 5.559305 -0.658417 6.164395  
 17.C 5.295260 -0.759727 4.751773  
 18.C 3.216507 -0.280011 3.223119  
 19.H 2.629079 -1.209668 3.142685  
 20.H 3.892268 -0.236032 2.362411

21.H 2.517308 0.560998 3.139641  
22.C 2.026844 0.658669 6.016095  
23.H 1.313339 -0.175415 6.109200  
24.H 1.697545 1.285982 5.179040  
25.H 1.958586 1.259150 6.931044  
26.C 4.177178 -0.010013 8.304594  
27.H 3.773388 -0.942652 8.731579  
28.H 3.472534 0.795484 8.546533  
29.H 5.118406 0.208998 8.824204  
30.C 6.802185 -1.139294 6.853634  
31.H 6.714812 -2.207025 7.110561  
32.H 6.985609 -0.587818 7.783525  
33.H 7.686332 -1.019731 6.216191  
34.C 6.170442 -1.461461 3.760954  
35.H 5.990704 -2.548986 3.792112  
36.H 7.233747 -1.295493 3.969627  
37.H 5.970896 -1.122719 2.739129  
38.C 8.172879 3.435299 2.173306  
39.C 7.051678 4.285946 1.827634  
40.C 6.018289 3.455558 1.268831  
41.C 6.485012 2.107228 1.290029  
42.C 7.815506 2.086280 1.852106  
43.C 9.515128 3.905351 2.653826  
44.H 10.183649 4.125436 1.805208  
45.H 10.006996 3.148592 3.277151  
46.H 9.429892 4.819895 3.253200  
47.C 7.045765 5.786744 1.853601  
48.H 7.431040 6.192084 0.903550  
49.H 7.673055 6.181854 2.661829  
50.H 6.033502 6.184779 1.997598  
51.C 4.733083 3.941051 0.664096  
52.H 4.865144 4.198117 -0.400144  
53.H 4.361068 4.837463 1.175504  
54.H 3.944460 3.180425 0.723331  
55.C 5.802820 0.954908 0.617967  
56.H 6.072630 0.918539 -0.450809  
57.H 4.710335 1.037352 0.671395



58.H	6.095383	-0.009009	1.050952
59.C	8.734774	0.900451	1.900314
60.H	9.323382	0.812286	0.971566
61.H	8.181610	-0.038368	2.024646
62.H	9.445722	0.976575	2.732636

**16b**

1.Rh	6.766429	3.489795	8.729300
2.Rh	6.007495	3.281949	6.100244
3.B	6.660843	5.105549	6.992101
4.B	7.878087	4.258407	5.933105
5.B	7.831587	2.817520	7.054303
6.H	6.065415	6.136070	6.791261
7.H	8.320567	4.464479	4.833884
8.H	8.488220	1.800745	6.983721
9.H	7.034645	5.129517	8.252250
10.H	7.907600	5.423970	6.556101
11.H	8.810747	3.738215	6.672825
12.H	5.383770	3.314550	7.738685
13.C	5.012144	1.467954	5.084883
14.C	5.804607	2.201314	4.147206
15.C	5.231248	3.535515	4.022674
16.C	4.072748	3.604613	4.868009
17.C	3.965278	2.348722	5.548407
18.C	6.535958	1.766922	10.086426
19.C	5.578879	2.737657	10.617382
20.C	6.290187	3.886435	10.998669
21.C	7.715050	3.648489	10.737987
22.C	7.863506	2.308122	10.255979
23.C	4.104727	2.502747	10.755408
24.C	5.733553	5.134107	11.618933
25.C	8.823734	4.573931	11.151549
26.C	9.148129	1.561797	10.059151
27.C	6.214962	0.350160	9.710222

28.C 6.9333382 1.656326 3.322031  
29.C 5.658120 4.583825 3.037150  
30.C 3.109571 4.752040 4.958253  
31.C 2.856591 1.954877 6.479451  
32.C 5.160756 0.015766 5.433512  
33.H 3.879823 1.949221 11.681627  
34.H 3.709523 1.913250 9.918948  
35.H 3.545441 3.445502 10.790714  
36.H 5.855790 5.119474 12.714309  
37.H 4.663361 5.249677 11.408151  
38.H 6.242582 6.032971 11.247604  
39.H 9.055765 4.449771 12.222411  
40.H 8.553747 5.626146 10.995122  
41.H 9.743960 4.379630 10.587477  
42.H 9.400451 0.979078 10.959980  
43.H 9.983157 2.243422 9.858120  
44.H 9.083958 0.865829 9.214561  
45.H 6.230411 -0.305809 10.596336  
46.H 6.940376 -0.045045 8.989066  
47.H 5.218376 0.269713 9.258460  
48.H 6.559912 1.242380 2.371452  
49.H 7.465079 0.855042 3.849173  
50.H 7.666517 2.435130 3.079650  
51.H 5.147220 4.440560 2.071227  
52.H 6.738223 4.547965 2.851000  
53.H 5.416583 5.592532 3.394361  
54.H 2.321405 4.672255 4.191517  
55.H 3.615057 5.714730 4.812761  
56.H 2.613913 4.787980 5.936301  
57.H 2.017456 1.514320 5.917431  
58.H 2.466658 2.816830 7.033766  
59.H 3.189373 1.207235 7.209517  
60.H 4.560896 -0.620554 4.761933  
61.H 4.831110 -0.190342 6.459564  
62.H 6.204707 -0.311309 5.352962

17

1.Ir	5.227488	1.427010	5.457160
2.Ir	6.452436	2.943578	3.484679
3.B	4.847267	3.569454	4.678039
4.B	6.503127	4.324071	5.054878
5.B	7.190808	2.631938	5.412610
6.H	3.828568	4.118602	4.345588
7.H	6.965459	5.429760	4.961823
8.H	8.301642	2.327257	5.763442
9.H	4.424500	2.844391	5.834455
10.H	5.312418	4.474587	5.613555
11.H	7.030753	3.803604	6.144178
12.H	6.383977	2.092421	6.464544
13.C	3.957113	-0.170537	4.539389
14.C	3.419408	0.179034	5.834589
15.C	4.403378	-0.124788	6.843416
16.C	5.567397	-0.656905	6.163029
17.C	5.290675	-0.705943	4.752012
18.C	3.187566	-0.184243	3.254644
19.H	2.615333	-1.121192	3.154411
20.H	3.854642	-0.105129	2.390549
21.H	2.475665	0.648074	3.202285
22.C	2.025337	0.670616	6.088615
23.H	1.334085	-0.181180	6.189040
24.H	1.663624	1.297665	5.264965
25.H	1.965434	1.259734	7.011367
26.C	4.206698	-0.048135	8.328401
27.H	3.785407	-0.990612	8.714258
28.H	3.518887	0.760234	8.603567
29.H	5.153526	0.130089	8.852014
30.C	6.800347	-1.196294	6.825581
31.H	6.681444	-2.270168	7.040633
32.H	7.005628	-0.687324	7.774831
33.H	7.683342	-1.079053	6.186235
34.C	6.150002	-1.388858	3.735428
35.H	5.955233	-2.473948	3.741149

36.H	7.216215	-1.239478	3.939742
37.H	5.945089	-1.019468	2.726417
38.C	8.127315	3.413690	2.098916
39.C	6.988159	4.252907	1.769053
40.C	5.943122	3.401688	1.256327
41.C	6.422394	2.054045	1.281015
42.C	7.767168	2.048330	1.809851
43.C	9.492202	3.898288	2.491590
44.H	10.111946	4.084371	1.599036
45.H	10.016118	3.162050	3.113469
46.H	9.439504	4.834291	3.060535
47.C	6.977910	5.752879	1.761089
48.H	7.349208	6.136557	0.796984
49.H	7.614642	6.165061	2.552917
50.H	5.966242	6.149827	1.910696
51.C	4.635645	3.862494	0.682614
52.H	4.731740	4.080656	-0.394020
53.H	4.279680	4.775827	1.174447
54.H	3.853174	3.101980	0.796834
55.C	5.738819	0.899633	0.613654
56.H	5.983602	0.890323	-0.461585
57.H	4.646958	0.963431	0.692890
58.H	6.058591	-0.067570	1.017661
59.C	8.704113	0.875625	1.831510
60.H	9.280732	0.811236	0.893384
61.H	8.166196	-0.072581	1.949090
62.H	9.424223	0.950609	2.655709